Mitigation of Microbially Induced Concrete Corrosion: Quantifying the Efficacy of Surface Treatments using ASTM Standards

by

Oluwafisayomi Folorunso

Submitted in Partial Fulfillment of the Requirements

for the Degree of

Master of Science in Engineering

in the

Civil and Environmental Engineering Program

YOUNGSTOWN STATE UNIVERSITY

August 2023

Mitigation of Microbially Induced Concrete Corrosion: Quantifying the Efficacy of Surface Treatments using ASTM Standards

Oluwafisayomi Folorunso

I hereby release this thesis to the public. I understand that this thesis will be made available from the OhioLINK ETD Center and the Maag Library Circulation Desk for public access. I also authorize the University or other individuals to make copies of this thesis as needed for scholarly research.

Signature: _____ _____

Oluwafisayomi Folorunso, Student — Date

Approvals:

_____ _____

Dr. Richard A. Deschenes, Thesis Advisor — Date

_____ _____

Dr. Holly Martin., Committee Member — Date

_____ _____

Dr. Byung-Wook Park, Committee Member — Date

_____ _____

Dr. Salvatore A. Sanders, Dean of Graduate Studies — Date

Abstract

Concrete wastewater infrastructure is facing a significant issue known as microbially-induced concrete corrosion (MICC), causing major concern within the wastewater industry. Various methods have been explored to reduce economic loss and service interruptions. The aim of the present study was to evaluate the resistance of mortars exposed to sulfate attack, acid attack, and MICC to develop mitigation strategies to increase the service life of wastewater infrastructure. This study provides valuable insights for developing sustainable solutions to mitigate MICC in wastewater infrastructure, including recommendations for future research.

A biocidal admixture, acid resistance coating (ARC), and a sodium nitrite ($NaNO_2$) treatment were tested in accordance with ASTM standards. These results indicated that the treatments were ineffective in mitigating sulfate or acid attack on direct exposure to chemical sulfates or acids. A further aim of the present study was to compare the performance of mortar and surface treatments exposed to MICC (ASTM C1894) with the performance of the same materials when exposed to chemical sulfate attack (ASTM C1012) or acid attack (ASTM C1898). Nasr (2021) and Sapkota (2022) previously examined the efficacy of a series of surface treatments against MICC using an accelerated chamber test. The biocidal admixture and ARC treatments were found to have similar sulfate and acid resistance trends, consistent with the previous studies. However, the $NaNO_2$ treatment produced different results, with a lower effectiveness in inhibiting sulfate attack but a higher effectiveness in maintaining strength after acid exposure.

Acknowledgments

I want to express my sincere gratitude to all those who have contributed to the successful completion of this research.

Firstly, I would like to thank my supervisor, Dr. Richard Deschenes, for his guidance, support, and valuable suggestions throughout the research. His expertise and constant encouragement have been instrumental in shaping this work.

I would also like to thank my thesis committee members, Dr. Holly Martin and Dr. Byung-Wook Park, whose insights and feedback have improved the quality of this work.

I am sincerely grateful to Dr. Bhargavi Mummareddy, Ray Hoff, and Dr. Bharat Yelamanchi for their invaluable assistance and contributions throughout the various stages of my research.

I am also grateful to Youngstown State University, which provided me with the necessary resources and facilities to conduct this research.

Lastly, I thank my family and friends for their unwavering support and encouragement throughout my academic journey. Their love and support have been my source of strength.

Once again, I express my gratitude to all who contributed to the successful completion of this project.

Table of Contents

List of Figures

List of Tables

List of Abbreviations

ARC	Acid-Resistant Coating
ASOM	Acidophilic Sulfur Oxidizing Microorganisms
CAC	Calcium Aluminate Cement
CH	Calcium Hydroxide
H_2S	Hydrogen Sulfide
H_2SO_4	Sulfuric Acid
MIC	Microbially-Induced Corrosion
MICC	Microbially-Induced Concrete Corrosion
Na_2SO_4	Sodium Sulfate
$NaNO_2$	Sodium Nitrite
RH	Relative Humidity
SMD	Standard Mean Difference
SOB	Sulfur Oxidizing Bacteria
S_2O_3	Thiosulfate
SRB	Sulfur Reducing Bacteria

1. Introduction

1.1. General Overview

Microbially-induced corrosion (MIC), or specifically, microbially induced concrete corrosion (MICC), is one of the numerous durability issues that can impact the service life of wastewater infrastructure. The MICC mechanism has impacted wastewater systems around the world for many years, and a sustainable solution is yet to be developed. There have been numerous studies on alternatives to cement, novel cement systems, and ways to extend the service life of wastewater infrastructure (Narasimhan, 2016; Azzouz et al., 2017; Li et al., 2018). It is crucial to identify effective mitigation strategies for managing and inhibiting MICC in concrete wastewater infrastructure. These strategies will help to reduce lifecycle costs and enhance resilience.

There have also been numerous studies on the application of surface treatment, such as chemical, antimicrobial, or beneficial biofilm coatings, to existing sewer surfaces (Sand et al., 1997; Hewayde et al., 2007; Ganigue et al., 2010; Jiang et al., 2016). A lack of standardized test methods makes direct comparisons of the efficacy of treatments difficult. The development of ASTM standards for sulfate attack (ASTM C1012), acid attack (ASTM C1898), and MICC (ASTM C1894) provides a series of widely accepted methods for quantifying the efficacy of mortars and treatments for preventing or mitigating MICC. However, each of the standards purports to measure different properties of concrete and is not directly comparable to the performance of concrete when exposed to MICC. For example, ASTM C1012 and C1898 were developed for testing the resistance of concrete to specific chemical attacks, while ASTM C1894 is a guide for testing resistance to microbially induced concrete corrosion. To understand the relationship between these test methods and the holistic performance of mortars and treatments on exposure to MICC results from all three test methods were considered herein. Rather than a

qualitative comparison between the results, the standard mean difference (SMD) was used to provide a numerical, statistical comparison.

In the present study, specific stages of MICC were simulated using chemical sulfate and sulfuric acid attack. Sulfate and sulfuric acid attack were simulated following ASTM C1012 *Standard Test Method for Length Change of Hydraulic-Cement Mortars Exposed to a Sulfate Solution* and ASTM C1898 *Standard Test Method for Determining the Chemical Resistance of Concrete Products to Acid Attack*, respectively. The results were then compared to those of a previous study conducted by Nasr (2021) and Sapkota (2022), in which MICC was simulated using an accelerated chamber test, as specified in ASTM C1894 *Standard Guide for Microbially Induced Corrosion of Concrete Products*.

1.2. Problem Statement

Numerous studies have been dedicated to evaluating the efficacy of treatments aimed at mitigating MICC. Notably, Zhang et al. (2008), O'Connell et al. (2010), and Wu et al. (2020) have conducted significant research in this area. These studies have made valuable contributions to our understanding of MICC mitigation strategies and have provided insights into the effectiveness of various treatment approaches. Despite the continuous evaluation of these treatments over time, none has demonstrated long-term efficacy. The present study explores the feasibility of utilizing ASTM C1012 and C1898 test methods as a reliable means of evaluating treatments for MICC, providing a faster and more efficient alternative to Nasr (2021) and Sapkota (2022) laboratory simulations. Furthermore, the study aims to develop a more durable mitigation method for in-situ concrete. For this purpose, mortar samples were tested based on ASTM standards to simulate the second and third stages of MICC.

1.3. Objective

This research, therefore, aims to assess the sulfate and sulfuric acid resistance of mortars coated with surface treatments and to compare the results to those previously reported by Nasr (2021) and Sapkota (2022). In this present study, the acid and sulfate attack experiments were based on ASTM C1012 and ASTM C1898. The results previously reported by Nasr (2021) and Sapkota (2022) were based on ASTM C1894. The results from acid and sulfate attacks will be compared to those from the laboratory simulation study in which the same surface treatments were evaluated.

1.4. Scope

The scope of this research was to assess the effectiveness of three surface treatments (biocide, ARC, and $NaNO_2$) in mitigating MICC within mortar specimens. The performance of these treatments was assessed over six months through exposure experiments. The results from the accelerated ASTM C1012 and ASTM C1898 tests are provided for the three treatments studied and indicate variations compared to the more extensive simulation outlined in ASTM C1894. It is crucial to bear in mind that each test method utilized in evaluating concrete properties measures distinct aspects and cannot be directly compared to one another. To assess the resistance of concrete to certain chemical attacks, ASTM standards C1012 and C1898 are utilized, while ASTM C1894 is a guide for testing the resistance of concrete to MICC. Therefore, it is unlikely that a direct numerical comparison can be made between the results obtained from ASTM C1012 and C1898 and those from ASTM C1894, except with the use of statistical comparisons such as the SMD.

2. Literature Review

The relevant, previous research carried out on the corrosion process will be reviewed herein as a basis for the present study, which centered on the acid and sulfate attack that occurs during the later stages of MICC (ASTM C 1894, 2019). The effect of MICC has been explored both in the laboratory and in situ (Sand and Bock, 1991; Islander et al., 1991; Monteny et al., 2000; Okabe et al., 2007).

2.1. Mechanism of Concrete Corrosion

To understand the relationship between acid attack, sulfate attack, and the MICC mechanism, a summary of the current research to date on biogenic and chemical corrosion mechanisms will be provided herein.

A comprehensive understanding of MICC is provided by multiple studies, which emphasize the crucial role of sulfur oxidizing bacteria (SOB) in the corrosion process. The case studies presented by Grengg et al. (2015, 2017) highlight this role, explaining the significance of these bacteria in concrete deterioration. Notably, the model proposed by Grengg et al. (2017) unveils a detailed perspective on how acidophilic bacteria contribute to the rapid progression of MICC. The findings of Grengg et al. (2017) align with the experimental findings of Jiang et al. (2016) and Li et al. (2019), which explicitly underscore the fast-paced nature of the corrosion process incited by these bacteria. Building on this, Li et al. (2017) delved into the environmental aspects by delineating the ecology of acidophilic and neutrophilic microorganisms within sewer environments. Their exploration contributed to the broader comprehension of the living conditions of these bacteria, further aiding in the understanding of their role in MICC. Together, these studies provide a more holistic view of MICC, combining detailed microbiological insight with practical observations of concrete deterioration. The focus on sulfur oxidizing and

acidophilic bacteria across these works reinforces their crucial role in MICC and the importance of targeting these organisms in mitigation strategies.

The MICC process is typically divided into three stages, as first summarized by Islander et al. (1991). The corrosion process is visualized in **Figure 2.1**.

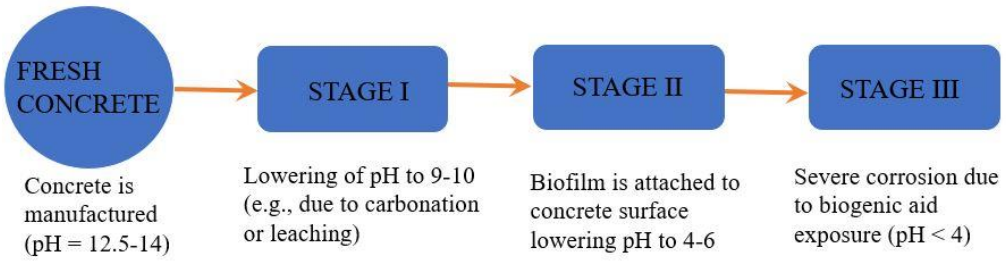

Figure 2.1 Three-Stage Process of MIC of Concrete (Recreated from ASTM C1894-19).

The corrosion process relates to the sulfur cycle that begins with sulfur-reducing bacteria (SRB) within the wastewater or biofilm. SRB reduces sulfates and oxidizes biodegradable organic carbon within the wastewater leading to dissolved hydrogen sulfide (H_2S) and carbon dioxide (CO_2) within the wastewater. Finally, the gases equilibrate between the wastewater and the atmosphere above the water line (Alexander et al., 2013).

The pH level of the concrete surface plays a critical role in the corrosion process, as it governs the chemical and biological reactions. Fresh concrete normally exhibits a surface pH ranging from 12 to 13, which acts as a deterrent for bacterial growth (Montenegro et al., 2012). During the initial phase of deterioration, abiotic acid-based reactions, such as carbonation and simultaneous sulfuric acid attack, are the prominent cause of neutralization, decreasing the pH from 12-13 to approximately 9-10. The formation of sulfuric acid at this stage stems from the abiotic oxidation of H_2S, facilitated by moisture on the concrete surface (Islander et al., 1991; Okabe et al., 2007; Nielsen et al., 2008). These oxidized sulfur species serve as nutrients for the subsequent colonization of sulfur-oxidizing bacteria (SOB) and the generation of biotic acids in the later stages of corrosion. Initially, there is minimal concrete material loss. However, the

calcium hydroxide (CH) leaching and the precipitation of sulfates salts, such as gypsum or ettringite, may occur at the corrosion interface (Islander et al., 1991; Sun et al., 2008; Neville, 2011).

MICC is a complex process influenced by several factors, including the activity of neutrophilic sulfur oxidizing bacteria (NSOB) and the production of sulfuric acid (Islander et al., 1991; Joseph et al., 2012). As the surface pH of concrete decreases, it creates an environment favorable for the colonization of NSOB strains (Islander et al., 1991; Joseph et al., 2012). These bacteria oxidize sulfur compounds to sulfuric acid (H_2SO_4) in the presence of moisture (Islander et al., 1991).

Continuous microbiological activity plays a crucial role in the deterioration of concrete by promoting the production of biogenic H_2SO_4, which leads to acidification and dissolution of the cementitious matrix (Islander et al., 1991). The acidification process results in the further production of sulfate salts and the reduction in both the pH of the concrete surface and the pore solution to approximately 9 (Joseph et al., 2012). The acidification process leads to loss of material as the stability of cementitious hydrates is compromised as the pH decreases below 11 (Grengg et al., 2015).

Unlike typical sulfate attack, the low pH along the concrete surface in MICC has the potential to obstruct the development of ettringite and the typical cracking associated with expansion (Grengg et al., 2015). Instead, oversaturation of the pore solution leads to the formation of gypsum, bassanite, or anhydrite and additional loss of cementitious material (Grengg et al., 2015; Jiang et al., 2016).

The microbial activity and subsequent acidification during the second stage of MICC result in the dissolution of the cementitious material, reduction of surface and pore structure pH, and the

formation of sulfate salts and expansive minerals. These processes contribute to the deterioration and loss of material in concrete structures affected by MICC (Grengg et al., 2015).

As the corrosion process continues, the concrete is further acidified until the surface pH reaches approximately 4, and the corrosion process transitions into the third stage. At this point, acidophilic sulfur oxidizing bacteria (ASOB) dominates the biofilm (Jiang et al., 2016; Li et al., 2017). The acidification of the biofilm is accompanied by deterioration due to the cementitious materials becoming unstable in acidic conditions (ASTM C1894, 2019). This acidic environment contributes to material loss and significantly increases corrosion rates (Grengg et al., 2015).

2.2. Sulfate Attack

Sulfate attack is a chemical process leading to the deterioration of concrete. A sulfate attack occurs when sulfates present in the surrounding environment react with the hydrates of Portland cement, leading to the formation of expansive compounds (Neville, 2011; Ejaz et al., 2013; Poole & Sims, 2016). These expansion products exert pressure on the concrete matrix, causing it to crack, spall, and deteriorate (Neville, 2011).

Sulfate attack occurs through physical and chemical mechanisms. De Schutter and Audenaert (2004) described the dual nature of the sulfate attack, physical and chemical. While the chemical aspect involves reactions with concrete constituents, the physical aspect involves the crystallization pressure of salts formed due to the sulfate attack. The physical mechanism happens when expansive or hygroscopic salts form within the pores of the concrete, inducing pressure, cracking, and deterioration (Skalny et al., 2002). A chemical attack occurs when cement hydration products and sulfate ions react to form expansive compounds like ettringite and gypsum that lead to deterioration (Neville, 2004).

Tikalsky et al. (2004) noted that the two primary sources of sulfates are typically groundwater and soil. The type of sulfate, concentration, and other environmental factors affect the severity and rate at which sulfate attack occurs. The severity of a sulfate attack is influenced by several factors, including the concentration and type of sulfate, permeability, and composition of the concrete, and environmental conditions such as temperature and moisture. For example, Suryavanshi et al. (1996) found that tricalcium aluminate (C_3A), a component of cement, is more susceptible to sulfate attack than other components. Ramlochan et al. (2000) detailed the effect of additives that inhibit sulfate attack and found that fly ash and silica fume mitigate sulfate attack due to their pozzolanic properties, which bind aluminum from C_3A in insoluble reaction products, reducing its availability for reaction with sulfates.

In a study, Lothenbach et al. (2008) suggested that sulfate attack is a multifaceted process, where the mechanism depends on the presence of other ions and environmental conditions. The phenomenon of sulfate attack is intricate and can be affected by several factors, such as the composition of the cement and additives used to the specific environmental conditions in which the concrete is situated.

There are similarities and differences between the chemical sulfate attack, as tested according to ASTM C1012, and the sulfate attack, which occurs during the second stage of MICC. In sewer networks, the presence of dissolved sulfides in wastewater plays a critical role in the initiation of MICC. Sulfates in the waste stream are typically converted to aqueous sulfides (H_2S) by SRB. These dissolved sulfides are essential for the formation of hydrogen sulfide (H_2S), which serves as a key precursor in the corrosive processes that affect concrete structures. During MICC, NSOB/ASOB oxidizes sulfides to sulfates, leading to sulfate attack within the concrete microstructure and the deposition of sulfate salts (gypsum or ettringite) along with the formation

of expansive sulfate salts. As the sulfate attack occurring during MICC is like the chemical sulfate attack, this mechanism can be simulated and accelerated through direct exposure to a sulfate solution, according to ASTM C1012.

2.2.1. ASTM C1012 Sulfate Attack

Sulfate exposure plays a significant role in the deterioration of concrete structures. The reaction occurs between sulfate ions and the hydration products of cement, causing expansion, cracking, and eventual deterioration. ASTM C1012 serves as a valuable standard test method for assessing the susceptibility of concrete or mortar to sulfate attack by measuring the length change of the specimens. The ASTM C1012 test involves the preparation of concrete or mortar bars that are then stored in a sulfate solution. The length changes of the samples are monitored over time, for at least 180 days, but often up to one or two years. By analyzing the rate and extent of expansion, ASTM C1012 provides a reliable measure of resistance to sulfate exposure of the material, enabling informed assessments of its susceptibility to sulfate attack (ASTM C1012, 2018).

The ASTM C1012 test has been used in various research studies for predicting the sulfate resistance of cementitious materials. It is a crucial test for evaluating new cement types or concrete mixtures designed to resist sulfate attacks (Santhanam et al., 2003). However, some researchers have pointed out that while ASTM C1012 is useful, it may not fully replicate all conditions seen in the field. For instance, the method may not completely account for variables such as varying sulfate concentrations, alternate attack mechanisms (like acid attack), or the influence of other environmental factors (Irassar, 2009).

ASTM C1012 has also been critical to understanding and mitigating sulfate attacks on concrete. Researchers have used ASTM C1012 to assess the efficacy of supplementary cementitious materials (SCMs), like fly ash and slag, in enhancing sulfate resistance (Neville, 2011; Mehta

and Monteira, 2014; ASTM C1012, 2018). The results show that the proper incorporation of SCMs can enhance the ability of concrete to withstand sulfate attack (Thomas et al., 2012). While some limitations exist, this standard continues to be a useful tool for developing more durable concrete mixtures.

2.3. Acid Attack

The first stage of MICC involves the abiotic conversion of hydrogen sulfide (H_2S) gas into sulfuric acid (H_2SO_4). During the second stage, the concrete structure undergoes biogenic sulfuric acid corrosion (Islander et al., 1991). The process outlined below demonstrates how acid attack mimics the second and third stages of MICC as per ASTM C1898. Initially, abiotic (chemical) neutralization occurs via sulfide oxidation and concrete carbonation before bacterial colonization. Carbonation is a chemical process that occurs when carbon dioxide interacts with CH in the hydrated cement. Further, contact with wastewater, typically lower pH than concrete, causes CH to leach, reducing surface pH. Finally, the abiotic and biogenic acid attack leads to the neutralization and acidification of the cement structure (Islander et al., 1991).

The acid attack mechanism, which occurs during chemical sulfuric acid attacks, can be used to simulate aspects of the third stage of MICC. Oxidation of H_2S by SOB generates a biogenic sulfuric acid attack in Portland cement concrete. To simulate the final stage of MICC, the cement structure is exposed directly to the sulfuric acid solution, resulting in the dissolution of cement hydrates and the formation of sulfate salts.

Chemical acid and biogenic (or microbial) acid attacks differ in their mechanisms. A chemical attack involves direct contact between concrete and an acidic solution, typically sulfuric acid, leading to the deterioration of the cementitious hydrates (Neville, 2004). In contrast, a biogenic acid attack involves a biological process. Microorganisms, particularly SOB, generate sulfuric

acid responsible for the attack (Sand and Bock, 1991). This biological process adds complexity to the attack mechanism, as it is affected by microbial growth rates, substrate availability or solubility, and environmental conditions, such as temperature, humidity, and pore solution pH (Gu et al., 2001). In addition, there may be differences in the attack patterns between chemical and biogenic acid attacks. MICC often results in more uneven and localized corrosion due to the distribution of microorganisms, whereas chemical attack typically results in more uniform corrosion (Okabe et al., 2007).

2.3.1. ASTM C1898 Acid Attack

A comprehensive understanding of the acid attack on concrete and its prevention can be gained through the application of the ASTM C1898, a test method that provides a procedure for evaluating the chemical resistance of concrete on exposure to acid (Taheri et al., 2020; Zaw, 2021). ASTM C1898 contains a standard method to assess the resistance of concrete to acid attack, which simulates the acid attack that occurs during stage three of the MICC (O'Connell et al., 2012).

As such, ASTM C1898 serves as a useful tool in studying the acid resistance of concrete, with researchers utilizing this method to develop concrete that can resist various forms of chemical attack (Alexander and Mindess, 2005; Neville, 2011; ASTM C1898, 2020). The test procedure involves subjecting concrete specimens to a specified concentration of sulfuric acid, then measuring changes in the mass and flexural strength of the concrete and the appearance of the samples and test solution. The results provide valuable insight into the ability of the concrete mixture to withstand harsh environments, thereby informing suitable material selection and design (ASTM C1898, 2020).

Several studies highlight the importance of ASTM C1898 in understanding acid attacks on concrete. For instance, Bertron et al. (2014) employed ASTM C1898 to examine the resistance of different cementitious materials to acid attack, demonstrating how variations in material compositions can influence resistance levels. Their research emphasized the value of ASTM C1898 in providing comparative results for different materials, informing more resistant and sustainable concrete production. Similarly, the research conducted by Gruyaert et al. (2016) utilized ASTM C1898 to examine the impact of mineral additions on the acid resistance of concrete. They found that additions like fly ash and slag could enhance resistance, emphasizing the role of ASTM C1898 in supporting concrete improvement strategies. In the field of MICC, Liu et al. (2017) used ASTM C1898 to explore the resistance of various concretes to microbiologically produced sulfuric acid, providing insights into the efficacy of different concrete mixtures in resisting microbial attack.

2.4. Simulation of Microbially-Induced Concrete Corrosion (MICC)

Simulating the biophysical conditions present during MICC in the laboratory has proven challenging. The conditions present in sewer environments must be understood first before simulated environments can be developed. In their research, Grengg et al. (2015) carried out a detailed examination of MIC in a combined sewer network. Their findings revealed the significant impact of acidophilic bacteria in the rapid advancement of MICC. Similarly, Grengg et al. (2017) emphasized the crucial role played by acidophilic bacteria in sewer environments, contributing to the occurrence of MICC. Li et al. (2017) investigated the acidophilic microorganisms responsible for corroding concrete sewer environments and identified several microbial species that contributed to the acidification of concrete.

These observations indicated that MICC is a complex biophysical process, with acidophilic bacteria playing a central role in accelerating concrete corrosion in sewer environments. Understanding these processes and the microorganisms involved is critical as it guides the development of new construction materials and protective measures to combat MICC. Aspects of MICC can be simulated by direct exposure to acidophilic bacteria, as in benchtop immersion tests. These laboratory tests offered controlled environments for studying MICC, allowing for the manipulation of several factors, such as bacterial concentrations, temperature, and exposure time to accelerate and simulate real-world MICC conditions (Islander et al., 1991). Accelerated chamber testing is another method used in the literature to simulate MICC conditions found in wastewater environments (Joseph et al., 2010, 2012; ASTM C1894, 2019; Nasr, 2021; Sapkota, 2022).

2.4.1. ASTM C1894 MICC

The standard guide ASTM C1894 stands as a pivotal framework in managing MICC, which has been the focus of numerous academic and industrial research (Fava and Little, 2015; Li et al., 2018; ASTM C1894, 2019). The guide provides an overview of MICC, its effects, and potential testing and mitigation methods, which have been instrumental in standardizing research efforts and industry practices.

The ASTM C1894 specification offers three approaches to evaluate the efficacy of concrete when exposed to MICC. These include (1) Accelerated Chamber Tests, (2) Benchtop Biogenic Immersion Tests, and (3) Acid Immersion Tests (such as ASTM C1898). These test methods each simulate aspects of the MICC mechanism. The accelerated chamber test serves as a crucial means of assessing the resistance of concrete to MICC, thereby contributing to the preservation of concrete structures over the long term. According to ASTM C1894, conducting accelerated

chamber tests can be challenging due to the generation of highly toxic H_2S gas. Hence, it might be more feasible to employ benchtop biogenic immersion and acid immersion tests to assess the efficacy of treatments. It should be noted that these tests only replicate individual stages of corrosion and do not replicate the actual field conditions encountered in wastewater environments.

Simulation studies, such as those conducted by Jin et al. (2015) and Li et al. (2017), have used a comprehensive approach to examine the multifaceted nature of MICC. This approach, later outlined in ASTM C1894, incorporates both the biological processes and the resulting physical and chemical changes in concrete. The literature surrounding MICC often aligns with the protocols outlined in ASTM C1894. One of the critical factors emphasized in the ASTM C1894 guide is the role of SOB in MICC, which has been investigated in studies like Okabe et al. (2007). Such research underscores the importance of understanding the biological processes driving MICC.

Several researchers focus on testing and mitigation strategies for MICC as outlined in ASTM C1894. Wang et al. (2016) leveraged these guidelines to test various environmental conditions affecting the severity of MICC. Research on mitigation techniques, such as that by Esnault et al. (2013), follows the recommendation of the guide for developing and testing preventative measures.

Nasr (2021) and Sapkota (2022) conducted an experimental study to assess the performance of concrete under accelerated conditions simulating MICC. The accelerated chamber test method was utilized to compare different surface treatments. The evaluation of performance was based on measurements of surface pH and sulfide uptake rate (SUR). The research included four surface treatment methods: epoxy mastic, acid-resistant coating (ARC), biocidal admixture, and

surface-applied $NaNO_2$. Changes in surface pH and SUR were monitored over two years of exposure, and the four surface treatment methods were evaluated (Sapkota, 2022). Treatments that inhibit changes in pH and colonization of SOB were found to be most effective. The results underscore the importance of acid attack resistance and buffer capacity in mitigating the onset of MICC, which prevents the onset of later stages.

ASTM C1894 is employed in the assessment of material suitability for infrastructure that is exposed to wastewater environments. ASTM C1894 plays a role in evaluating various concrete types and surface treatments in terms of their resistance to MICC (Park and Tansel, 2019). However, it is crucial to acknowledge that this standard guide does not fully replicate all the conditions encountered in real-world scenarios, including the presence of fluctuating environmental factors like temperature and moisture.

The ASTM C1894 has been instrumental in developing mitigation strategies for MICC. These strategies range from the use of novel concrete compositions to surface treatments, and all are focused on enhancing the ability of concrete to withstand acid corrosion and bacterial activity. (Sun et al., 2016). In summary, ASTM C1894 serves as a central reference point for literature concerning MICC, providing a standardized framework for investigating the phenomenon, testing its effects, and developing mitigation strategies.

2.5. Mitigation of MICC

MICC is a multifaceted process encompassing various stages. It starts with the adsorption of gaseous H_2S onto the concrete surface, which occurs through physical means. Subsequently, the oxidation of sulfide to sulfuric acid is facilitated by chemical and biogenic processes. Finally, this is followed by the acid attack reaction between the sulfuric acid and the concrete (Sun et al., 2015). Methods to prevent or mitigate sulfate attacks have been studied extensively. These range

from using sulfate-resistant cement to incorporating various additives, like pozzolans or antimicrobial chemicals. These additives can help to reduce the permeability of the concrete or modify concrete composition (Thomas et al., 2012). The two prevailing methods for mitigating ongoing MICC in the wastewater industry are as follows:

- Dosing of wastewater with iron salts, magnesium hydroxide, nitrate, or sodium hydroxide inhibits the reduction of sulfates to H_2S. The limitation of this method is that dosing the wastewater with chemicals may contaminate wastewater, have limited efficacy, and increase maintenance costs (Sun et al., 2015; Jiang et al., 2018; Sharma et al., 2018).
- For concrete treatments, corrosion-resistant paint or surface treatment reduces permeability. Biocidal treatments inhibit or deactivate SOB, thereby inhibiting the conversion of sulfides to sulfuric acid. The limitation of this method is the difficult surface preparation and application and the frequency of reapplication (Neville, 2004; Isgor and Razaqpur, 2006; Joseph et al., 2013; Sun et al., 2015).

2.5.1. ASTM C1904 Antimicrobial Additives

Erbektas et al. (2019) conducted an assessment to determine the effectiveness of antimicrobial additives in mitigating the biogenic acidification of simulated wastewater solutions caused by microorganisms. Erbektas et al. (2019) tested the efficacy of antimicrobial products on SOB in solutions with varying pH levels and bacterial activity. Following ASTM C1904, Erbektas et al. (2019) conducted experiments to simulate the MICC mechanism. The experiment involved introducing acid-producing microorganisms to concrete specimens and exposing them to conditions conducive to biogenic acidification. The researchers monitored various parameters such as pH, sulfate concentrations, and weight loss to assess the corrosive effects of the acidification process on the concrete. The product under investigation demonstrated effective

prevention or delay of biogenic acidification in the presence of high bacterial populations and activity when pH levels were above 6. Additionally, it showed efficacy in mitigating the acidification caused by low to moderate bacterial populations and activity when pH levels were above 4 (Erbektas et al., 2019).

The use of ASTM C1904 in the study allows for consistent and comparable evaluations of antimicrobial additives. The researchers introduced several types of additives to concrete specimens and assessed their effectiveness in inhibiting microbial activity and mitigating acid-induced concrete corrosion. The standard helps establish a systematic approach for evaluating the performance of antimicrobial agents and concrete products under simulated MICC conditions.

The ASTM C1904 standard has been instrumental in simulating and analyzing the mechanisms of MICC. ASTM C1904 establishes a standard for quantitatively assessing the performance of antimicrobial additives used in concrete to inhibit biogenic acidification, the primary mechanism of deterioration in MICC (Erbektas et al., 2019). This standard effectively mirrors the conditions under which MICC occurs in the real world, creating a platform to test the efficacy of various additives in preventing or reducing the rate of corrosion.

One of the key features of ASTM C1904 is that it incorporates the simulation of biofilm formation, an important aspect of MICC, in its assessment protocol. As detailed by several researchers, such as Jin et al. (2015), and Li et al. (2017), the presence and growth of biofilms significantly contribute to MICC, and ASTM C1904 simulation methods allow for the accurate testing of how antimicrobial additives affect biofilm development.

Furthermore, Wang (2016) demonstrated that ASTM C1904 facilitates the evaluation of the durability and integrity of concrete samples after exposure to biogenic acidification. By

simulating the chemical interactions that typically occur in MICC, the standard provides a reliable platform for assessing the long-term effects of MICC on concrete products.

Through the development of controlled, reproducible MICC environments, ASTM C1904 offers a robust methodology for testing and evaluating the performance of antimicrobial additives in concrete. By simulating key aspects of the MICC mechanism, the standard supports the development of more resilient concrete products and treatments. Overall, ASTM C1904 serves as a valuable tool for researchers studying MICC and antimicrobial additives.

2.6. Surface pH Mapping

Grengg et al. (2019) began by highlighting the significance of pH in concrete corrosion processes and the limitations of traditional methods in capturing pH distribution across the concrete surface. The researchers introduce high-resolution optical pH imaging as a non-destructive technique that can overcome these limitations by providing spatial pH measurements. The experimental work involves the development and application of a pH-sensitive indicator film based on a combination of poly(styrene) and bromothymol blue. The film is attached to the concrete surface, and changes in color are recorded using an optical imaging setup. By correlating the observed color changes with known pH values, the pH distribution across the concrete surface can be determined.

The researchers conducted a series of experiments to validate the accuracy and reliability of the optical pH imaging technique. Concrete samples were subjected to chemically corrosive environments, including sulfuric acid solutions of varying concentrations, and monitored the pH distribution over time. The results of the study substantiate the ability of the optical pH imaging method to accurately capture pH changes at a high spatial resolution.

Furthermore, Grengg et al. (2019) discuss the potential applications of high-resolution optical pH imaging in concrete research and practice. Emphasis was on the usefulness of assessing the effectiveness of protective coatings and evaluating the performance of repair materials. The technique can provide valuable information on the local pH conditions, enabling targeted interventions to mitigate concrete corrosion.

The study by Grengg et al. (2019) presents high-resolution optical pH imaging as a promising technique for studying concrete deterioration in chemically corrosive environments (Foorginezhad et al., 2020). The method offers improved spatial resolution and non-destructive assessment capabilities, enabling a better understanding of pH distribution and changes in concrete. The research opens avenues for further investigations and applications of optical pH imaging in the field of concrete corrosion and protection.

2.7. Summary of Test Methods

Comparing mitigation methods can be better achieved by utilizing the test methodologies of ASTM C1012, ASTM C1898, and ASTM C1894 rather than relying solely on the test methodology of ASTM C1894. These additional ASTM standards provide more suitable approaches for evaluating and comparing the effectiveness of various mitigation techniques (Erbektas et al., 2019; ASTM C1894, 2019; ASTM C1904, 2020). The ASTM C1898 specification was published during the work of Nasr (2021) and was not included in the earlier work. Therefore, the results of acid and sulfate attack exposure will be compared to the earlier work, which relied only on accelerated chamber simulation of MICC (ASTM C1894, 2019).

3. Experimental Methods

3.1. Introduction

In this present research, the sulfate and sulfuric acid resistance of mortars coated with surface treatments (biocide, acid-resistant coating, and $NaNO_2$) were evaluated following ASTM C1012 and ASTM C1898, which are discussed in **Section 3.3** and **Section 3.4**. Nasr (2021) and Sapkota (2022) evaluated the same treatments and conducted a long-term simulation of MICC using an incubation chamber and accelerated testing following ASTM C1894. The results from ASTM C1012 and ASTM C1894 test methods were compared with those from the long-term simulation study (ASTM C1894, 2019), as discussed in **Section 3.5**. Additional microscopy studies of samples from Nasr (2021) and Sapkota (2022) were conducted in the present research to determine the extent of acid and sulfate attacks, as discussed in **Section 3.5.2**.

3.2. Experimental Design

A summary of the test matrix from the present study and from Nasr (2021) and Sapkota (2022) is provided in **Table 3.1,** along with the specimen dimensions and a number of test specimens. Specimens were prepared and treated with epoxy mastic, acid-resistant coating (ARC), biocidal admixture, or surface-applied $NaNO_2$, with additional samples prepared as control samples.

Table 3.1 *Test matrix and sample dimensions.*

	ASTM C1012 Sulfate Attack		**ASTM C1898 Acid Attack**		**ASTM C1894 MICC Accelerated Chamber**
	Bars (1 x 1 x 11 in.)	Cubes (2 in.)	Beams (2 x 2 x 8 in.)	Cubes (2 in.)	Coupons (4 x 3 x 2 in.)
control	6	9	12	12	10
Epoxy*	0	0	0	0	10
ARC	6	9	12	12	10
biocide	6	9	12	12	10
$NaNO_2$	6	9	12	12	10
Total	**24**	**36**	**48**	**48**	**50**

*Epoxy was not **included** in the present study.

In the statistical analysis, significance was established if the probability that the difference between means occurred by chance was less than 0.05. The results are shown in **Table 4.1**, **Table 4.2**, and **Table 4.3**. If the p-value is less than 0.05, it means that the difference between the treatment group and the control group is not due to chance. This analysis, in combination with the experimental results, provides a comprehensive understanding of the effectiveness of different protective treatments against several types of attacks.

3.3. ASTM C1012 Sulfate Attack

The MICC experiment conducted by Nasr (2021) and Sapkota (2022) utilized simulated MICC conditions to accelerate deterioration. While this method better represents the conditions found in wastewater environments, it does not differentiate the sulfate or acid attack resistance of the concrete, which occurs during the second and third stages of MICC. To understand how concrete performs when subjected to sulfate attack, mortar bars were immersed in a Na_2SO_4 solution. The test procedure is explained in detail in **Section 3.3.1** below, including the casting and curing of the bars according to ASTM C1012. The section also detailed the surface treatment and exposure conditions of the mortar bars.

3.3.1. ASTM C1012

The standard test method for the determination of length change of hydraulic-cement mortars exposed to a sulfate solution is detailed in ASTM C1012. Mortar bar specimens were prepared based on the ASTM C1012 specification. The process for batching and casting the mortar bars was based on the method of ASTM C109. To measure the compressive strength, 2 in. (50 mm) cubes were made from the concrete batch and tested prior to immersing the bars in the sulfate solution.

The mortar bars were molded according to the standard test method of ASTM C157. Immediately after molding, the bars were covered and cured at 95±5 °F for 24 hours. Subsequently, after the initial curing, the bars were removed from the molds, and compression strength was checked following the test method of ASTM C109 to determine a mean strength, which should be 3000±150 psi. Once the desired strength was achieved, mortar bars were subjected to sulfate attack through immersion. The dimensional changes were assessed at specific intervals of 7, 14, 21, 28, 56, 91, 105, 122, and 183 days for all three surface treatment techniques.

3.3.1.1. Materials and Treatments

Various apparatus, reagents, and materials were used for the experiment in accordance with the ASTM standards. The apparatus included a mixer, cube molds, bar molds, comparator, weights, glass graduates, tamper, pH meter, stainless-steel gauge studs based on ASTM C490 specification, and containers for initial curing and the sulfate solution immersion. The reagents included deionized water and sodium sulfate, which were mixed to produce a sulfate solution. For solution preparation, deionized water was used with a pH between 6.0 to 7.5. Anhydrous sodium sulfate (Na_2SO_4) was used. A mixture of a sulfate solution containing 50 g of Na_2SO_4 was mixed into 900 mL of water, which was further diluted with deionized water to make 1.0 liters of the solution. The solution was mixed 24 hours before use and stored at 73.5±3.5 °F to allow the proper dissolution of the sodium sulfate powder. Before each use of the solution, the pH was confirmed to be between 6.0 and 8.0. To ensure an adequate solution volume, a specific ratio of sulfate solution to mortar bars was achieved by mixing an appropriate quantity of the solution in the storage container, which resulted in a mixture with four volumes of solution for every volume of bars. Designated glass beakers were used to mix the solution.

The materials used herein included standard graded sand, as specified in ASTM C778, and Type I/II Portland cement. **Table 3.2** below is a summary of the graduation of the sand used, which adheres to the Standard Sand Requirement prescribed in ASTM C778.

Table 3.2 *Standard Sand Requirement.*

Sieve	% Passing	% Retained	Weight (g)
16	100	0	0.0
30	96	4	199.6
40	60	36	1796.2
50	30	30	1496.9
100	4	26	1297.3
Pan	0	4	199.6
Total		**100**	**4989.5**

A portable concrete mixer was used for all mixing, and 163.5 in^3 of mortar was batched at a time. The final batching ratios and weight are summarized in **Table 3.3**.

Table 3.3 *Batching Weight.*

Constituents	W (g)	Ratio	Batch (lbs)	Volume (ml)
Cement	1814	-	4.00	-
Sand	4990	2.75	11.00	-
Water	880	0.485	1.94	880
Biocide	-	-	-	15
Volume Required	**163.5 (0.0946)**	**in^3 (ft^3)**		

For each treatment listed in **Table 3.1**, twelve cubes were batched in accordance with ASTM C109, and six bars were batched following ASTM C490. Aerosol lubricant was sprayed directly on the interior faces of the molds to prevent corrosion of metallic molds and facilitate the removal of the mortar after casting. Then the concrete mortar was poured into each mold in two layers. To ensure proper compaction, each layer was manually tamped eight times using a plastic tamper. After the second layer was tamped, the surface was troweled for consistency.

The concrete was cured for 23.5±0.5 hours in a metallic, corrosion and heat resistant container placed in an oven maintained at 95±5 °F. After demolding, two cubes were tested in compliance with ASTM C109 to determine if the compressive strength was within the required range of 3000±150 psi. If the compressive strength was below 2850 psi, the concrete was cured until the compressive strength fell within the required range.

The treatments were applied after curing was completed, except for the biocidal admixture, which was added to the fresh concrete following the recommendation of the manufacturer. The ARC was applied in two layers to the mortar bars within 30 minutes intervals before immersion in the sulfate solution. The $NaNO_2$ was sprayed on the mortar bars, which were placed in an air-tight bag for 24 hours before being submerged in the sulfate solution.

3.3.1.2. Exposure Conditions

For immersion, four plastic containers with an internal volume of three liters were used. The containers were resistant to the sulfate solution. Each container housed one set of bars (the number of bars used for each treatment is summarized in **Table 3.4**). The volume of the container was sufficient to contain six bars without touching the sides of the container and to contain a solution-to-mortar bar volume ratio of 4:1. Further; the containers were sealed to prevent the sulfate solution from evaporating while the bars were being stored (**Figure 3.1**). The storage temperature was 73.5±3.5 °F.

Figure 3.1 *Mortar bars in containers covered and sealed to prevent evaporation and stored in an environmental chamber (Photo by Oluwafisayomi Folorunso).*

The length comparator met the specifications of ASTM C409. At 7, 14, 21, 28, 56, 91, 105, 122, and 183 days of exposure to sulfate solution, the change in length was measured by means of a length comparator, as shown in **Figure 3.2** below, based on ASTM C490.

Figure 3.2 *Length Check with Length Comparator (Photo by Oluwafisayomi Folorunso).*

***Table 3.4**. Concrete specimens and their exposure conditions.*

Number of bars	Exposure Conditions (Treatment)
10	control
5*	biocide
4*	ARC
6	$NaNO_2$

*1 or 2 bars broke during testing

3.3.1.3. Analytical Method

The length change at each age for each treatment was determined using ***Equation 1***.

$$\Delta L = \frac{L_x - L_i}{L_g} \times 100 \qquad \textbf{Equation 1}$$

Where:

ΔL = Change in length at age x, %

L_x = Comparator reading of specimen at age x

L_i = Initial comparator reading of specimen

L_g = Nominal gauge length or 10 in. as applicable

Length change values for each bar to the nearest 0.001% and averages to the nearest 0.01% were calculated. The results were then plotted and compared, as discussed in **Chapter 4**.

3.4. ASTM C1898 Acid Attack

To simulate the third stage of the MICC, which is an aggressive acid attack (pH < 4), mortar bars were subjected to exposure to a sulfuric acid solution (H_2SO_4). The test procedure is explained in detail in **Section 3.4.1** below, including the casting and curing of the bars according to ASTM C1898. The section also includes details regarding surface treatment and exposure conditions.

3.4.1. ASTM C1898

The ASTM C1898 is a standard test method used to evaluate the impact of an acid attack, like the conditions which occur during stage three of the MICC mechanism. A chemical acid immersion test achieves acidification by immersion in sulfuric acid rather than through the

activity of microorganisms. Batching, curing, exposure, weight, and visual inspection of the test specimen are carried out and recorded. Mortar bars, treated with one of the treatments listed in **Table 3.1**, were exposed to acid attack by immersion. The flexural strength was then measured and recorded, as well as visual inspection and mass change for each test interval.

3.4.1.1. Materials and Treatments

Similar apparatus and materials as those used in **Section 3.3.1.1** were used for the experiment. The apparatus included a mixer, cube molds, bar molds, scale, graduated cylinders, tamper, pH meter, and containers for initial curing and acid immersion. The reagents used included 98% sulfuric acid and deionized water. For immersion of the test specimens, a test medium of sulfuric acid with a pH of 2.0 was used. The specimens were immersed with a solution-to-sample ratio of 4.2:1. To dilute the sulfuric acid, deionized water was used with a pH between 6.0 to 7.5. The concentrated acid was first diluted to produce a stock solution of molarity 0.05M. This 0.05M acid was further diluted to 0.005M in the exposure container weekly by adding deionized water. Before each use of the solution, the pH was confirmed to be between 1.8 to 2.1.

The concrete materials included standard graded sand, as specified in the specification of ASTM C778, and Type I/II Portland cement. The gradation for the sand is summarized in **Table 3.2** above based on the standard sand requirement in ASTM C778.

The batching and curing process was like that of **Section 3.3.1.1**. **Table 3.5** summarizes the mixture design and batch weights. After batching, the specimens were cured for 23.5±0.5 hours in a metallic, corrosion and heat resistant container, which was placed in an oven at 95±5 °F. The specimen was subjected to a curing period of 28 days under controlled conditions at a temperature of 73.5±3.5 °F.

The treatments were applied after curing, except for the biocidal admixture, which was added during mixing. The ARC was applied in two layers to the mortar bars within 30 minutes intervals and then cured for 24 hours before immersion in the acid solution. The $NaNO_2$ was sprayed on the mortar bars and placed in an air-tight bag for 24 hours before being placed in the acidic solution.

Table 3.5 *Batching Weight.*

	Mixture Design		**Batch (0.0204 yd^3)**	
	lb/yd^3	**ft^3/yd^3**	**lbs**	**ft^3**
Cement	1301	6.62	26.50	0.135
Fine	1952	11.5	39.80	0.235
Water	520	8.34	10.59	0.170
Air	0	0.54	0.00	0.011
Total	**3773**	**27.00**	**76.89**	**0.5508**

3.4.1.2. Exposure Conditions

A test medium of sulfuric acid, with a concentration of 0.005M (pH 2), was used for immersion. Three prisms with dimensions of 2 x 2 x 8 in. (50 mm x 50 mm x 200 mm (± 3 mm)) were used for each test interval of 1, 28, and 84 days. **Figure 3.3** below shows the sample bars immersed in the sulfuric acid solution.

After immersion, flexural strength was determined and recorded at select intervals, as well as a visual inspection of the specimen and the color and clarity of the test medium. During each test interval, the mass of the sample was determined, and the cleaning and air-drying process was carried out for 30 minutes prior to measuring the masses. The flexural strength test apparatus is shown in **Figure 3.4**.

Figure 3.3 *Mortar bars immersed in a sulfuric acid solution having a pH value of 2 (Photo by Oluwafisayomi Folorunso).*

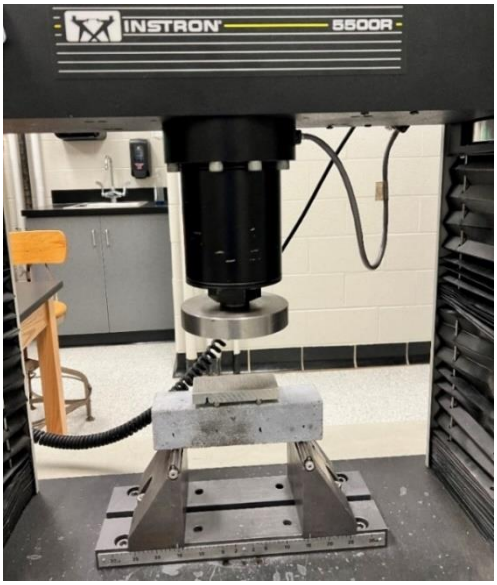

Figure 3.4 *Flexural Strength Test Set-up (Photo by Oluwafisayomi Folorunso).*

3.4.1.3. Analytical Method

The change in flexural strength (%) was determined per **Equation *2***.

$$\Delta R = \frac{S_1 - S_2}{S_1} \times 100\% \qquad \textbf{Equation 2}$$

Where:

S_1 = average flexural strength of specimens following the conditioning period

S_2 = average flexural strength of specimens following the test period

The changes in flexural strength with respect to time were then plotted and compared, as discussed in **Chapter 4.**

3.5. ASTM C1894 Accelerated Chamber Test

Nasr (2021) and Sapkota (2022) conducted an experimental investigation to evaluate the same treatments used in this present experiment in addition to epoxy mastic. Concrete coupons were cast, cured, and then treated before being exposed to accelerated MICC conditions. Three test methodologies were identified in quantifying MIC deterioration within the concrete. The test methods included sulfide uptake rate (SUR), surface pH, and Live/Dead staining (Nasr, 2021; Sapkota, 2022).

3.5.1. ASTM C1894

The experimental design implemented by Nasr (2021) and Sapkota (2022) involved the utilization of an incubation chamber designed specifically to simulate and expedite the aggressive conditions of MICC found in wet wells. The chamber was constructed using PVC and followed the procedures detailed by Joseph et al. (2010, 2012), providing a reliable and standardized setup. During the experiments, the test coupons were subjected to different exposure conditions to evaluate chemical corrosion and biogenic corrosion, as described in **Section 3.5.1.2**. The coupons were exposed to H_2S gas for chemical corrosion testing, while biogenic corrosion testing involved exposure to both H_2S gas and wastewater in the accelerated chamber test. These distinct exposure conditions were designed to simulate and assess the effects of specific corrosive agents commonly encountered in real-world scenarios.

ASTM C1894 (2019) includes guidelines for accelerated chamber tests to evaluate the possibility of MICC in concrete products. To accelerate the corrosion process, the accelerated chamber tests involve exposing specimens to a controlled environment of elevated temperature and humidity,

along with SOB. The standard recommends using a range of test conditions to simulate various environmental conditions that the concrete product could experience. The tests should also include appropriate controls to ensure that any observed corrosion is due to microbial activity rather than other factors. The results of the accelerated chamber tests can be used to evaluate the susceptibility of concrete products to MICC and to develop mitigation strategies to prevent or reduce corrosion.

3.5.1.1. Materials and Treatments

In the conducted experiment, the concrete coupons employed had specific dimensions of 4 x 3 x 2 in. (length, breadth, and thickness) with a mortar mixture design, as summarized in **Table 3.6**.

Table 3.6 *Concrete coupon design mixture. (Nasr, 2021).*

	Weight (lbs./yd^3)	**Volume** (ft^3)	**Ratio**	**S.G.**	**A.C.**	**Weight** (lbs./batch)
Cement	1301	6.62	1.00	3.15	-	24.10
Fine Aggregate	1952	11.50	1.50	2.72	0.01	36.14
Water	520	8.34	0.40	1.00	-	9.64
Air	-	0.54	-	-	-	-

The experimental procedure involved the preconditioning of concrete coupons through exposure to H_2S gas for a duration of 20 weeks before the application of surface treatments. The surface treatments applied included epoxy, ARC, biocide, and $NaNO_2$ treatment. The epoxy mastic, known for its corrosion resistance properties, was applied as a protective coating in two layers on the top face of each coupon. This coating serves as a barrier, preventing the penetration of corrosive agents into the concrete. The ARC treatment, consisting of a mixture of sodium silicate, quartz flour, and slag cement, along with an activator, was applied as a two-layer coating using a paint roller. This treatment forms an acid insoluble coating on the concrete surface, reducing permeability and hindering the diffusion of acid and bacteria into the underlying cement.

The biocide treatment, which aims to limit the development and growth of biofilms, involved the addition of a microbiostatic admixture containing 3-(Trimethoxysilyl) propyldimethyloctadecyl ammonium chloride. The biocide was mixed into fresh Portland cement mortar and applied to the top of the coupons with a thickness of approximately 6 mm. For the $NaNO_2$ treated coupons, the concrete surface was treated by spraying an aqueous solution onto the coupons. This treatment serves to inactivate SOB and inhibit biofilm growth. These surface treatments were applied to the concrete coupons using specific methods and materials to enhance corrosion resistance and limit the detrimental effects of acid attack and microbial activity.

3.5.1.2. Exposure Conditions

To generate a controlled concentration of H_2S gas in the accelerated chamber test, sodium sulfide solution was added to sulfuric acid at a regulated rate. To maintain the desired gas concentration, a peristaltic pump was employed to control the flow of the solution into the acid. A fan was used to disperse the gas. Real-time measurements of H_2S concentration were taken using a portable data-logger. The system was programmed to maintain a consistent atmosphere with H_2S gas concentrations ranging from 50 to 150 ppm (Nasr, 2021).

3.5.1.3. Analytical Method

The rate of sulfide uptake, or SUR, by the surface of the concrete, is a function of the rate of oxidation of sulfides by chemical or biogenic processes. The SUR test requires monitoring the rate of H_2S uptake over an exposure period. To determine the SUR, the concrete specimen is exposed to a known quantity of H_2S gas, and uptake is measured. During the test, a gas-tight PVC chamber held the concrete, a data logger, a fan, and a beaker of acid for gas generation. To ensure safety, the test was conducted under a fume hood. The SUR was calculated by measuring the exposed surface area and determining the surface-specific SUR, as discussed by Nasr (2021).

Regular SUR tests were conducted to monitor changes in the rate of sulfide uptake as corrosion progressed (Nasr, 2021).

To further quantify the efficacy of MICC mitigating strategies in concrete, monitoring the surface pH is crucial. Nasr (2021) conducted monthly surface pH measurements using an Extech surface pH meter and ultrapure water. The surface of the concrete was cleaned before the pH was measured, and the average pH was calculated from three repeated readings.

Finally, the variation in SUR and surface pH over a two-year exposure period were plotted, and the results were reported in **Chapter 4** and analyzed to compare the efficacy of the treatment methods.

3.5.2. Imaging and Microscopy

At the conclusion of the experiments of Nasr (2021) and Sapkota (2022), two concrete coupons from each of the treatments and the control samples, as explained in **Section 3.5.2.2,** were sent for thin section preparation. First, the samples were air-dried, then impregnated with ultra-low viscosity epoxy. Next, a thin section was removed from the middle portion of the specimen. The sections were then attached to a glass slide and polished to a final thickness of approximately 0.001 in. (30 μm). Finally, the slides were carbon coated before imaging or SEM analysis.

3.5.2.1. Internal pH

In addition to thin sections, 0.2 in. thick cross-sections of the samples were prepared for internal pH measurements. The pH variation with depth from the exposed surface was determined using the pH-indicating pen, which indicates the pH of the substrate as a color on the scale shown in **Figure 3.5** below.

Figure 3.5 *A typical cross-section with the pH indicating line drawn on the sample with a pH Pen (Photos by Oluwafisayomi Folorunso).*

3.5.2.2. SEM Imaging

Next, the thin sections were imaged using a JEOL Jib-4500 in the Ward Beecher building at Youngstown State University. SEM images and EDS elemental mapping was conducted for thin sections from each treatment and the control. **Figure 3.6** below shows a typical thin section before placement in the SEM.

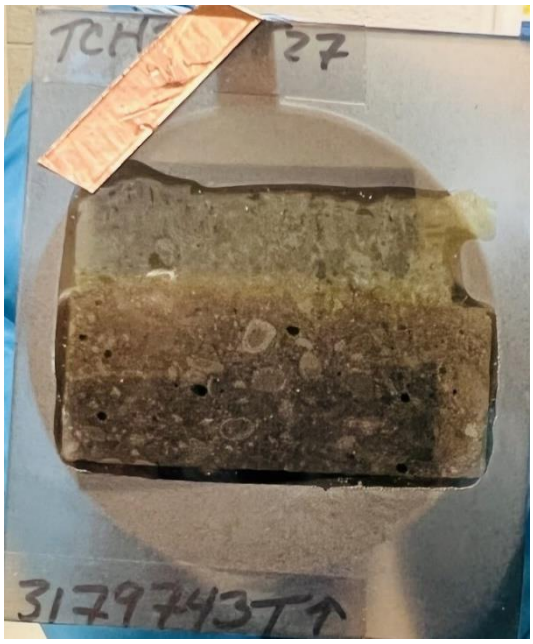

Figure 3.6 *Polished and Carbon-coated thin section of 1 in. (25 mm) diameter before being placed in EDS Chamber (Photo by Oluwafisayomi Folorunso).*

To identify each sample, the samples were coded as follows. Codes starting with an L indicate the lower coupons that were exposed to biogenic corrosion, while those with a U indicate the upper coupons exposed only to chemical corrosion, as indicated by the experimental design of Nasr (2021) and Sapkota (2022). The codes CT, ARC, EP, NAN, and BIO indicate the control, ARC, epoxy, $NaNO_2$, and biocide treatments, respectively.

Examples of SEM images at 22x magnification are summarized in **Section 4.4.2**. These images depict the ten samples and illustrate the corrosion interface between the intact concrete at the lower part of each image and the corroded material at the upper part.

4. Results and Discussion

The results obtained from the experimental investigation are summarized, analyzed, and discussed in this chapter. The results include ASTM C1012, ASTM C1898, a summary of ASTM C1894 from the works of Nasr (2021) and Sapkota (2022), and finally, the SEM and pH imaging.

To establish the statistical significance of the data, t-tests were performed to compare the mean values of each metric with that of the control. If the resulting p-value was found to be less than 0.05, it was considered to indicate a statistically significant difference, indicating that the treatment outperformed the untreated control.

4.1. ASTM C1012 Sulfate Attack

Recall, as discussed in **Section 3.3**, the ASTM C1012 test procedure involves exposing concrete specimens to a sulfate solution for 183 days and periodically measuring the length change of the concrete to assess the degree of sulfate attack. The results of ASTM C1012 testing are then used to evaluate the durability of concrete structures in sulfate-rich environments, such as wastewater treatment plants, sewer mains, marine structures, and roadways exposed to deicing salts. The test is also used to compare the performance of different concrete mix designs and additives in resisting sulfate attacks. The extent of sulfate attack on the concrete specimens, as indicated by length change, is summarized in **Section 4.1.1**. The degree of sulfate attack is classified into five categories (Mehta and Monteiro, 2014) as follows:

- No attack (insignificant): negligible expansion or deterioration observed.
- Mild attack: slight expansion and minor surface scaling.
- Moderate attack: expansion, cracking, and loss of bond between aggregate and paste.
- Severe attack: significant expansion, extensive cracking, loss of bond, and spalling.

- Very severe attack: extreme expansion, disintegration of the concrete, and potential structural failure.

The test results are used to classify the concrete as either resistant or susceptible to sulfate attack. Concrete is considered resistant to sulfate attack if the length change is less than 0.10% after exposure to the sulfate solution for 12 months. Significant expansion indicates the concrete may not be suitable for sulfate-rich environments.

4.1.1. Percent Strain

The percent strain for the mortar bars exposed to sulfate solution trended up over time, as summarized in **Figure 4.1** below. **Table 7.1** in the **Appendix** provides additional information on the percent strain data of the mortar bars collected over six months. Lower percentage strain means worse performance, while higher percentage strain means better performance.

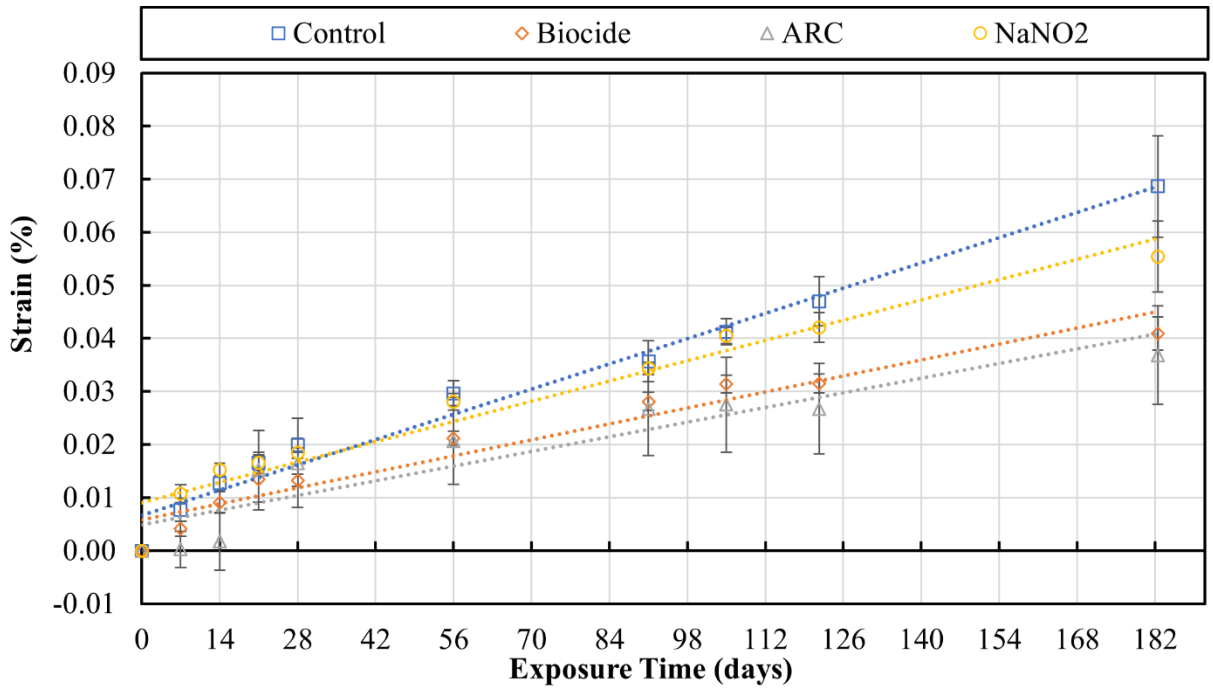

Figure 4.1 *Trendlines showing percent strain with respect to exposure time (days) for the control (n=10), biocide (n=5), ARC (n=6), and $NaNO_2$ (n=6) treatments.*

Based on the data summarized in **Figure 4.1**, each treatment showed distinct trends over the observed periods. The control sample had the greatest expansion, followed by the ARC, $NaNO_2$, and biocide samples.

The difference between the control and the biocide samples was statistically significant ($p < 0.05$). The difference between the control and the ARC samples was also statistically significant, indicating that the difference is due to something other than experimental or random error. However, the difference between the control and the $NaNO_2$ sample was not statistically significant. The t-test results are summarized in **Table 4.1**.

Table 4.1 *Summary of p-values from t-test for sulfate attack.*

	0	**7**	**14**	**21**	**28**	**56**	**91**	**105**	**122**	**183**
biocide	*0.000*	*0.011*	*0.009*	*0.108*	*0.000*	*0.000*	*0.003*	*0.000*	*0.000*	*0.000*
ARC	*0.000*	*0.003*	*0.005*	0.364	0.235	*0.044*	0.057	*0.015*	*0.002*	*0.000*
$NaNO_2$	*0.000*	*0.029*	*0.011*	0.495	0.059	0.161	0.274	0.319	0.056	*0.027*

$p < 0.05$ indicates statistical significance.

4.2. ASTM C1898 Acid Attack

The ASTM C1898 test method involved exposing concrete samples to a diluted acid solution for 84 days and measuring the changes in mass loss and flexural strength of the specimens. These measurements provide valuable insights into the acid resistance of concrete and its suitability for applications in acidic environments.

The results of the ASTM C1898 test can be expressed in terms of mass loss, flexural strength, or surface erosion. The test results serve as indicators of the resistance of concrete to acid attack. A significant mass loss, surface erosion, and reduction in flexural strength suggest that the concrete may not be suitable for use in acidic environments. A test result with significant mass loss or surface erosion and reduction in flexural strength indicates that the concrete is susceptible to acid attack and may not be suitable for use in acidic environments.

The results of the ASTM C1898 test are used to classify the degree of sulfuric acid attack on the concrete, according to the ASTM C1898 standard. The classification system ranges from *no attack* to *severe attack* as follows.

- No attack: a mass loss of less than 5% and a reduction in flexural strength of less than 10%.
- Moderate attack: a mass loss of 5-20% and reduction in flexural strength of 10-30%.
- Severe attack: a mass loss of more than 20% and reduction in flexural strength of more than 30%.

The mass loss and flexural strength reduction in the present study were less than 1%, indicating *no attack*. However, the study was carried out for 84 days; a more extended study period may yield a different result.

4.2.1. Mass Change

A summary of the percent mass change with respect to time is provided in **Figure 4.2**. Over time, all the treatments resulted in a decrease in the mass of the samples. The data reveals how each treatment performed differently over time. A lower percentage mass change means worse performance, while a higher percentage mass change means better performance.

Between day 1 and 28, the control group decreased the most (11.64%), while the ARC group decreased the least (3.83%). The biocide group (4.26%) and the $NaNO_2$ group (7.43%) decreased moderately over the same period. Between day 28 and 84, the $NaNO_2$ group decreased the most (33.01%), far outpacing the other groups. The control group also saw a substantial decrease (19.01%), while the ARC (10.10%) and biocide (8.91%) groups had modest decreases.

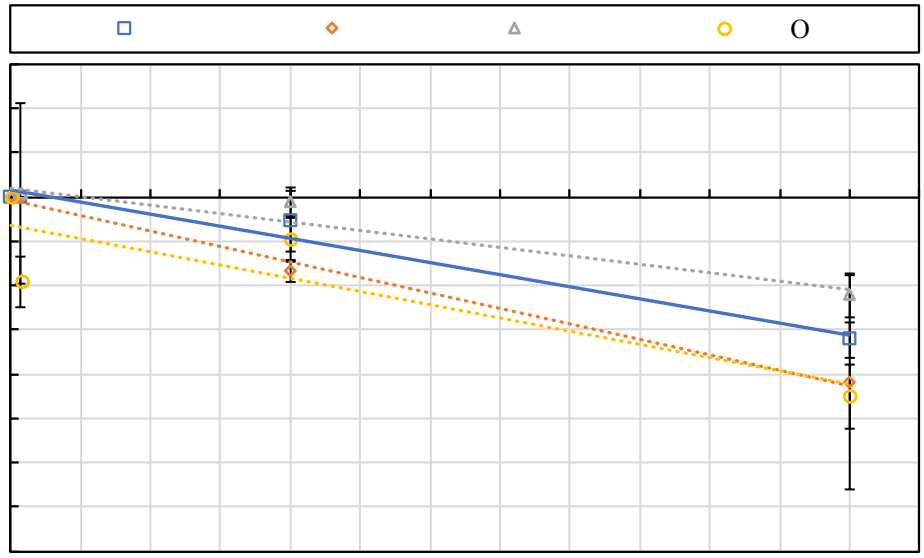

Figure 4.2 *Trendlines showing percentage mass change with respect to exposure time (days) for the control (n=3), biocide (n=3), ARC (n=3), and $NaNO_2$ (n=3).*

From day 1 to 84, the $NaNO_2$ group showed a decrease the most (42.84%), followed by the control group (32.92%). The biocide (13.55%) and ARC (14.31%) groups decreased less.

Based on **Table 4.2**, it is observed that the difference between the control group and the ARC group was not statistically significant, while the difference between the control and the other two treatments was statistically significant ($p < 0.05$). Thus, in terms of overall change, the $NaNO_2$ group showed the most substantial change, suggesting that $NaNO_2$ treatment may be less effective compared to other treatments or no treatment (control) while the biocide treatment is the most effective.

Table 4.2 *Summary of p-values from t-test for mass change.*

Time	**ARC**	**biocide**	**NaNO2**
28 Days	*0.047*	0.191	0.232
84 Days	0.287	*0.023*	*0.042*

$p < 0.05$ indicates statistical significance

4.2.2. Appearance of Specimens and Test Media

For the control samples, on day 1 of exposure, there was no difference in the appearance of the test medium or the appearance of the specimens. On day 28, the grey color of the concrete had given way to a sand-brown color, but there was a minor difference in the appearance of the medium. On day 84, there was a complete discoloration of the mortar bars to a sand-brown color, as shown in **Figure 4.5** below, and the appearance of the medium had changed to brownish color, as shown in **Figure 4.7.**

Day 1 **Day 28** **Day 84**

Figure 4.3 Appearance of control specimens after exposure to acid attack (Photo by Oluwafisayomi Folorunso).

For the samples batched with biocide, on day 1 of exposure, there was no difference in the appearance of the medium or the appearance of the specimen. On day 28, the grey color of the concrete had changed to a sand-brown color, and the edges of the bars had chipped, but there was a minor difference in the appearance of the medium. On day 84, there was a complete discoloration of the mortar bars to a sand-brown color, as shown in **Figure 4.4** below, and for the medium, as shown in **Figure 4.7**, the appearance had changed to a brownish solution.

Day 1 **Day 28** **Day 84**

Figure 4.4 *Appearance of biocide specimens after exposure to acid attack (Photo by Oluwafisayomi Folorunso).*

For the samples coated with ARC, on day 1 of exposure, there was no difference in the appearance of the medium or the appearance of the specimen. On day 28, the mortar bars had lost some of the coatings, as shown in **Figure 4.5** below. On day 84, the mortar bars had lost more of the coating, making the test medium milky, as shown in **Figure 4.7**.

Day 1 **Day 28** **Day 84**

Figure 4.5 *Appearance of ARC specimens after exposure to acid attack (Photo by Oluwafisayomi Folorunso).*

For the sample treated with $NaNO_2$, there was no difference in the appearance of the medium or the appearance of the specimen on day 1 of exposure. On day 28, the grey color of the concrete had given way to a sand-brown color, and the edges of the bars had chipped away, as shown in

Figure 4.6 below, but there was little difference in the appearance of the medium. On day 84, there was a complete discoloration of the mortar bars to a sand-brown color, and for the medium, as shown in **Figure 4.7**, the appearance had changed to a brownish solution.

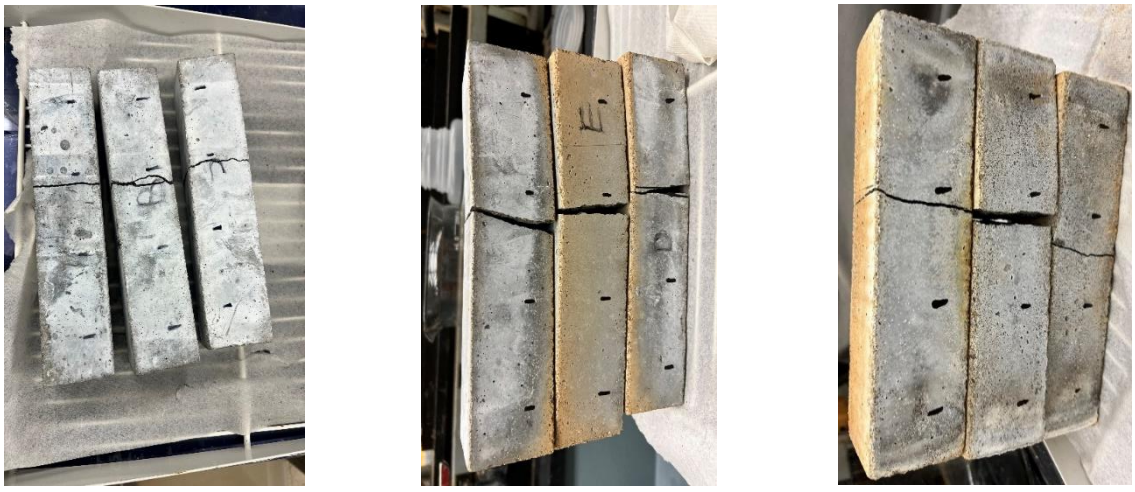

Day 1 **Day 28** **Day 84**

Figure 4.6 *Appearance of $NaNO_2$ specimens after exposure to acid attack (Photo by Oluwafisayomi Folorunso).*

The discoloration of the specimen and medium was more apparent for the control samples, followed by the $NaNO_2$, then the biocide, and the least apparent in the ARC.

control **$NaNO_2$** **ARC** **biocide**

Figure 4.7 *Appearance of Medium after 84 days (Photo by Oluwafisayomi Folorunso).*

4.2.3. Flexural Strength

A lower percentage flexural strength change means worse performance, while a higher percentage flexural strength change means better performance.

Figure 4.8 shows the trend in the average percent change in flexural strength. The control samples experienced a consistent increase in flexural strength across the test duration, totaling a 32.90% increase by day 84. The result establishes a benchmark for evaluating the treated samples.

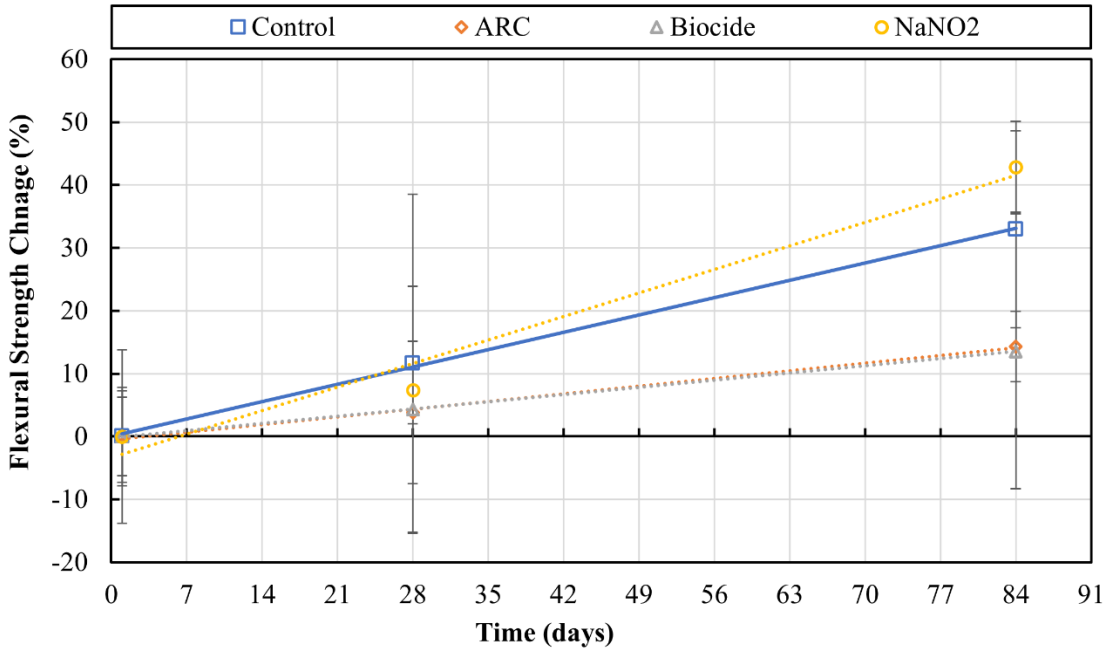

Figure 4.8 *Trendlines showing percentage flexural strength change with respect to exposure time (days) for the control (n=3), biocide (n=3), ARC (n=3), and $NaNO_2$ (n=3).*

The ARC and biocide samples exhibited less change as compared to the control. The ARC samples increased by 14.32%, about 56% less than the control. Similarly, the biocide sample also underperformed, with a 13.54% increase, approximately 59% less than the control. However, the $NaNO_2$ samples outperformed all other samples, with a 42.87% increase, representing a 30% increase over the control. This increase, primarily noted from Day 28 to Day 84, suggests a substantial long-term improvement in flexural strength due to $NaNO_2$ treatment. The $NaNO_2$ treatment emerged as the most beneficial in enhancing long-term flexural strength. The flexural strength of the ARC and biocide batches increased less across all periods compared to the control batch, indicating that their long-term effects were lesser. However, the $NaNO_2$

samples demonstrated a remarkable improvement in long-term performance, with the highest percentage increase from day 1 to 84, making it the most effective treatment among the four batches in this study.

The $NaNO_2$ batch demonstrated the highest percentage increase in flexural strength from day 1 to 84 (42.87%). This result is unexpected given that $NaNO_2$ is primarily intended to inhibit bacterial growth and should have minimal effect on acid resistance. The control batch also showed a consistent increase in flexural strength, albeit lower than the $NaNO_2$ batch, while the ARC and biocide samples underperformed. The performance of $NaNO_2$ in the test may indicate secondary effects or unintended consequences of the use.

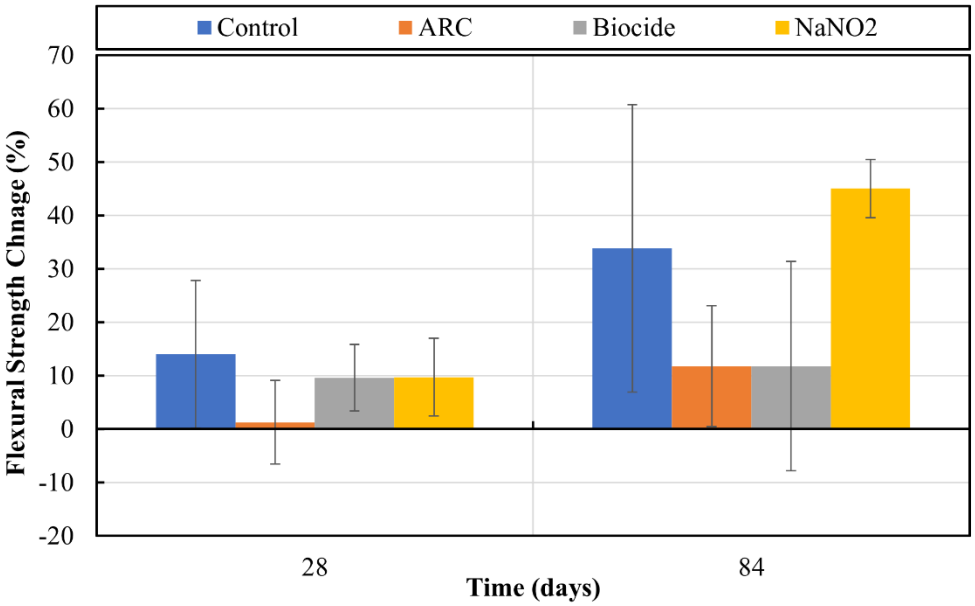

Figure 4.9 *Percentage flexural strength change with respect to exposure time (days) for the control (n=3), biocide (n=3), ARC (n=3), and NaNO2 (n=3).*

As depicted in **Table 4.3**, there was no statistically significant difference between the control group and the other treatments during the initial 28-day period (i.e., $p > 0.05$). However, from day 28 to 84, the ARC performed worse than the control samples by a statistically significant margin, while the difference between the control and other treatments was not statistically significant.

Table 4.3 *Summary of p-values from t-test for flexural strength change.*

Time	ARC	biocide	NaNO2
28 Days	0.193	0.386	0.372
84 Days	*0.034*	0.067	0.115

$P < 0.05$ indicates statistical significance.

4.3. ASTM C1894 MICC

In this section, the findings that were obtained through data collected during the experimental investigation by Nasr (2021) and Sapkota (2022) will be discussed, specifically, the results from surface pH and SUR testing of coupons that were exposed to chemical or biogenic corrosion will be examined. As reported by Sapkota (2022), exposure was separated into chemical and biogenic, as discussed in **Section 3.5.1**.

The incubation chamber used by Nasr (2021) and Sapkota (2022) was like the accelerated chamber test method discussed in ASTM C1894. The accelerated chamber test method is used to assess the resistance of concrete to MICC. The test involves exposing concrete samples to nutrient-rich wastewater and H_2S gas and then measuring the performance of samples after exposure. The performance of the concrete is quantified through a variety of methods, including mass change, surface pH, SUR, and microscopy.

In the study by Nasr (2021) and Sapkota (2022), the primary quantification methods were SUR, and the surface pH of the concrete samples was measured over time. The results were analyzed to evaluate the resistance of concrete and treatments to MICC and to determine whether the concrete is suitable for use in environments where microbial activity is likely to occur.

4.3.1. Sulfide Uptake Rate (SUR)

The SUR in concrete coupons was measured using an apparatus developed by Nasr (2021). The SUR of the treated and control samples were periodically measured, including those undergoing chemical and biogenic corrosion (Sapkota, 2022). The SUR test results from Sapkota (2022) are

summarized in **Figure 4.10** for chemical corrosion and **Figure 4.11** for biogenic corrosion. A higher SUR indicates worse performance, while a lower SUR indicates better performance. The SUR of all the treated coupons was lower than that of the control.

In terms of reducing SUR, the biocide treatment proved to be the most effective, followed by the $NaNO_2$ treatment with moderate effectiveness and the ARC treatment with the least effectiveness. Compared to the control, all treatments were successful in reducing SUR, but only the biocide treatment showed a statistically significant difference. **Figure 4.10** displays the trendlines indicating the rate of change of SUR for coupons exposed to chemical corrosion, according to Sapkota (2022).

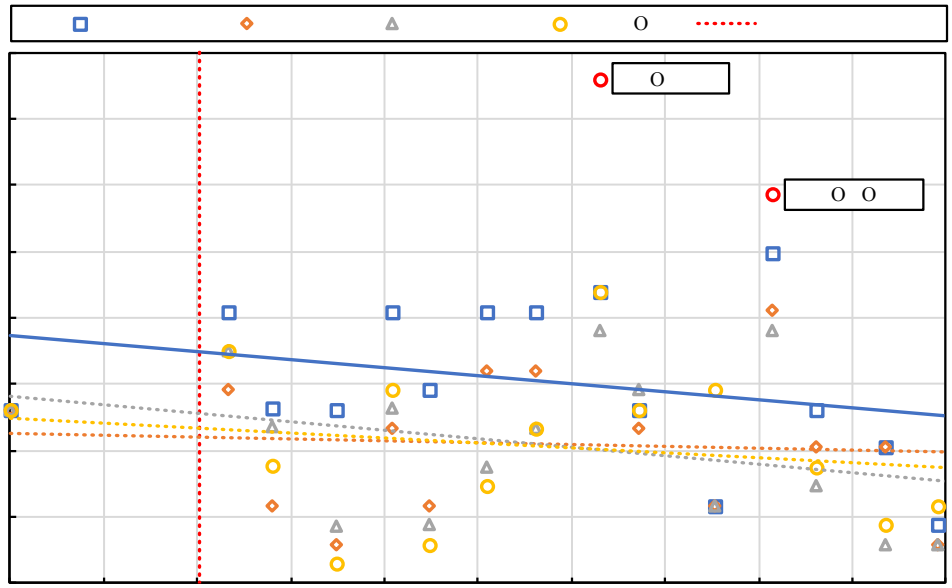

Figure 4.10 *Trendlines that show the rate of change of SUR for the coupons exposed to chemical corrosion (Sapkota, 2022).*

For chemical corrosion, among the three treatments studied, the biocide treatment effectively reduced SUR from 70.1 to 11.7 at a rate of -0.77/week, which was lower than the SUR of the control, which decreased from 81.8 to 17.6 at a rate of -0.85/week. The $NaNO_2$ treatment had a moderate effect on SUR. The SUR reduced at a rate of -0.61/week to decrease from 70.1 to 23.4.

The ARC treatment was the least effective in reducing SUR. The SUR decreased from 58.4 to 11.7 at a rate of -0.62/week, which was similar to that of the control.

The initial SUR of the control coupons exposed to chemical corrosion was 52.4, which increased to around 100 after two years. The initial SUR of the control coupons exposed to biogenic corrosion was also 52.4 but had increased to over 200 after two years. The results of this study suggest that biogenic corrosion can significantly accelerate the corrosion process of concrete. This is due to the biogenic corrosion conditions, which create an environment that is more favorable for the growth of sulfur-oxidizing microorganisms. These microorganisms produce acids that can corrode concrete. The results of this study suggest that biogenic corrosion is a significant threat to the durability of concrete. **Figure 4.11** shows the trendlines for coupons exposed to biogenic corrosion.

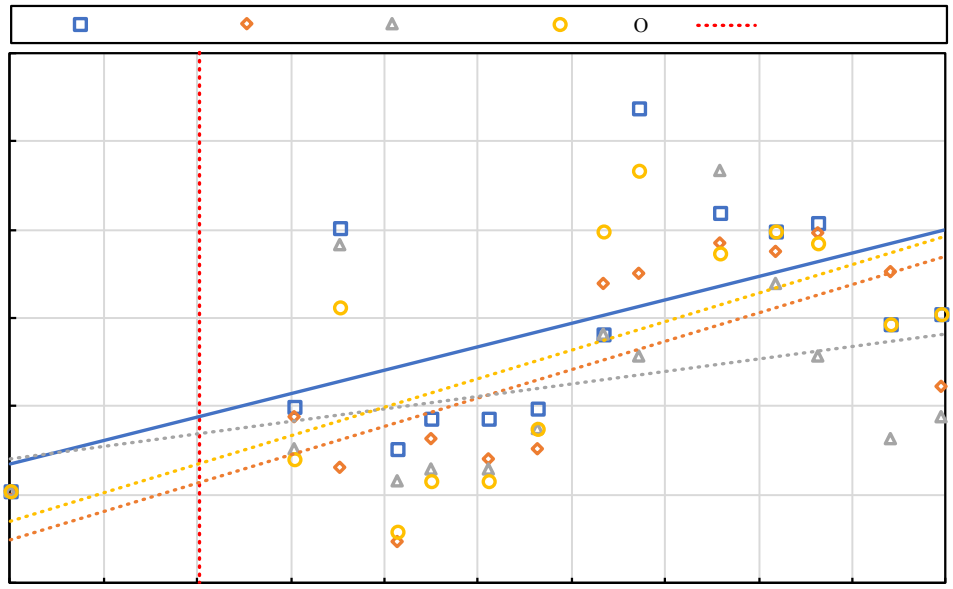

Figure 4.11 *Trendlines that show rate of change of SUR for the coupons exposed to Biogenic corrosion (Sapkota, 2022).*

The biocide treated coupons had the lowest SUR, increasing from 76.4 to 93.8 after two years at a rate of 0.25/week. The $NaNO_2$ treated coupons had a SUR comparable to the control,

increasing from 70.5 to 152 after two years at a rate of 1.18/week. The ARC treated coupons had a SUR increase from 94.1 to 111 at a rate of 0.25/week. The use of biocides or coatings can help to protect concrete from biogenic corrosion. For biogenic corrosion, the SUR of concrete coupons was measured after they were exposed to H_2S gas and wastewater. The results showed that the SUR of the coupons exposed to biogenic corrosion was significantly higher than the SUR of the coupons exposed to chemical corrosion, which was also observed by Sun et al., 2014. The statistical significance of the results was not measured as the SUR test was only conducted once for each treatment on each day due to the time required to conduct the test.

4.3.2. Surface pH

The surface pH results from Sapkota (2022) are summarized in **Figure 4.12** and **Figure 4.13**. Surface pH is important for monitoring concrete corrosion and reflects the pH of the exposed surface area as corrosion occurs. Lower pH means worse performance, while higher pH means better performance.

According to Sapkota (2022), monthly tests were conducted. For the chemical corrosion, it was observed that the control coupons consistently had the lowest surface pH. The coupons treated with ARC had a higher surface pH than the control. The surface pH of the coupons treated with ARC decreased from 10.3 to 5.5 over two years, a decrease of 4.8. The biocide coupons showed the highest surface pH levels among all treatments at all time points. The surface pH of the coupons treated with biocide decreased from 10.4 to 6.7 over two years, a decrease of 3.7.

The experimental results show that only the biocide and $NaNO_2$ specimens had surface pH higher than the control specimens by a statistically significant margin. On the other hand, the ARC specimens had only a slightly higher surface pH than the control specimens. According to the statistical analysis, differences in performance are considered significant if the 95%

confidence intervals of data points (error bars) overlap by less than 25%. These findings are illustrated in **Figure 4.12**. Based on the figure, all the treatments indicated a surface pH greater than the control by a statistically significant margin.

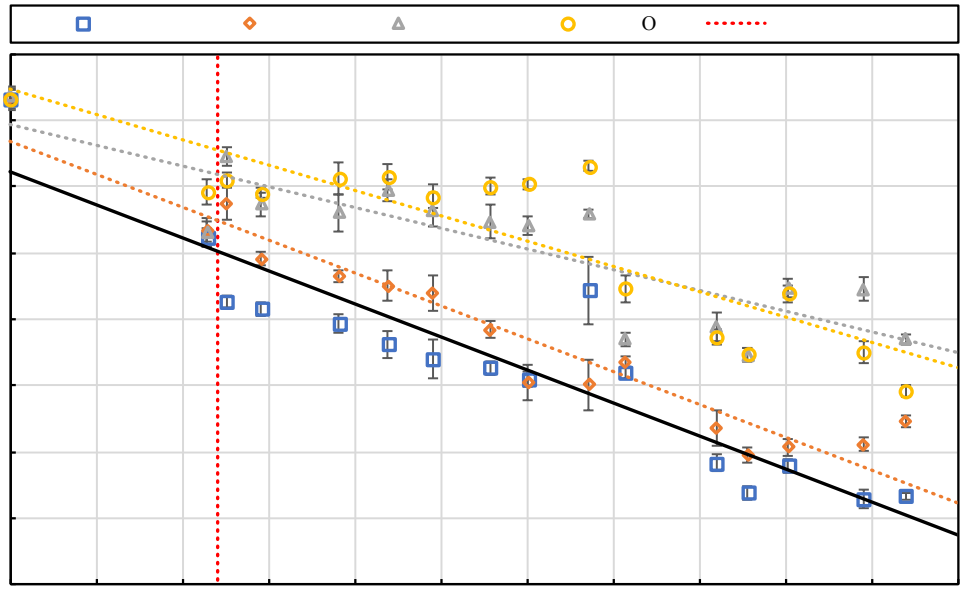

Figure 4.12 *Trendlines that show the rate of change in surface pH for the coupons exposed to chemical corrosion (Sapkota, 2022).*

For the biogenic corrosion, it was observed that the control coupons had the lowest surface pH throughout the experiment. The surface pH levels decreased from 10.4 to 2.9 over two years, indicating a decrease of 7.5. On the other hand, the ARC and biocide coupons had higher surface pH levels than the control coupons at all time points. The surface pH levels of the coupons treated with ARC decreased from 10.9 to 3.3 over two years, indicating a pH decrease of 7.6. Meanwhile, the surface pH levels of the coupons treated with biocide remained in the range of 10.4 to 3.5 over two years. Lastly, the $NaNO_2$ coupons had surface pH levels to those of the control coupons. Over a span of two years, the surface pH levels decreased from 10.6 to 3.1, indicating a significant pH decrease of 7.5.

The 95% confidence intervals for the data (error bars) were calculated and plotted in **Figure 4.13** to verify the statistical significance of the findings. Only the biocide specimens had a surface pH higher than the control specimens by a statistically significant margin, and this difference was only observed during weeks 25 to 60. None of the other specimens showed a statistically significant difference in surface pH compared to the control specimens. From weeks 25 to 60, biocide outperformed the control.

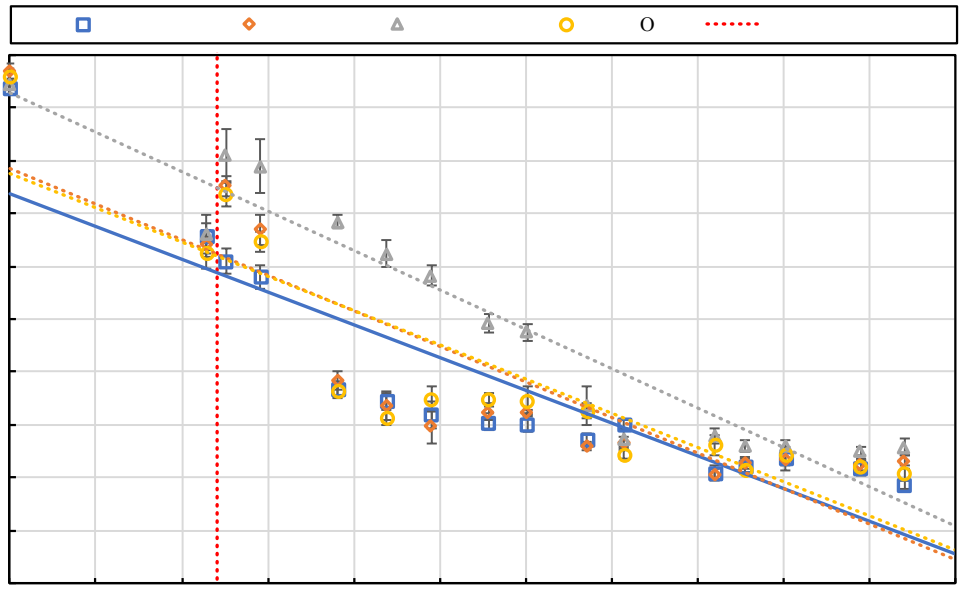

Figure 4.13 *Trendlines that show rate of change in surface pH for the coupons exposed to biogenic corrosion (Sapkota, 2022).*

4.4. Imaging and Microscopy

4.4.1. Internal pH of cross-sections

To better understand how the change in surface pH varied throughout the corrosion interface and further into the intact concrete, the variation of pH with depth from the exposed surface was determined by first cutting cross-sections from the various samples. The pH gradient was then determined using the pH-indicating pen, as shown in the images in **Figure 4.14** for the coupons

exposed to biogenic corrosion and **Figure 4.15** for the coupons exposed to chemical corrosion, respectively.

Figure 4.14 *Variation of pH in concrete cross-sections from control (CT), biocide (BIO), ARC, $NaNO_2$ (NAN), and epoxy (EP) samples exposed to biogenic corrosion for two years. Some severely corroded samples had a biofilm with a pH below 3 (orange portion of the vertical line), while the intact concrete had a pH above 11 (dark blue/purple portion of the vertical line) (Photos by Oluwafisayomi Folorunso).*

Figure 4.15 *pH Imaging of concrete cross-section from control (CT), biocide (BIO), ARC, $NaNO_2$ (NAN), and epoxy (EP) samples exposed to chemical corrosion for two years. The pH ranged between 10 to 14 through the intact concrete (Photo by Oluwafisayomi Folorunso).*

The images in **Figure 4.14** indicate that most specimens exposed to biogenic corrosion were severely corroded and had a biofilm with a pH below 3 (the orange portion of the vertical line). The lower pH indicates the concrete is corroded. The images in **Figure 4.15** show that the concrete cross-sections of the samples exposed to chemical corrosion are intact, as indicated by the dark blue/purple portion of the vertical line, with a pH range between 10 to 14.

The pH of concrete can change over time, depending on the environment in which it is exposed.

In the case of severely corroded concrete, the pH is typically much lower than in intact concrete. This is because microorganisms in the biofilm of the corroded concrete can oxidize sulfides to sulfuric acid as a byproduct of their metabolism.

The pH of the intact layer of the concrete (**Figure 4.14**) is due to the concrete being in an early stage of corrosion. The concrete has not yet been significantly damaged by the acids produced by the microorganisms, and the pH has not yet dropped below 10.

As the process of concrete corrosion progresses, the pH levels within the concrete decrease further. This decrease in pH exacerbates the deterioration of the concrete, resulting in a loss of mechanical performance. The corrosive environment created by microbial activity and chemical reactions contributes to the ongoing degradation of the concrete, posing a significant risk to the integrity and longevity of the structure.

The surface pH declined about twice as quickly in the biogenic corrosion-exposed coupons as in those exposed to chemical corrosion, as observed by Sapkota (2022). According to Sapkota (2022), the surface pH of control coupons subjected to biogenic corrosion decreased to approximately 3 within a span of two years, indicating the progression of corrosion due to microbial activity. The concrete was neutralized more quickly by continuous acid production resulting from biogenic corrosion (Li et al., 2020). During the active corrosion phase, which is stage three, the surface pH reached a stable level in the presence of biogenic corrosion. The rate of surface pH change was higher in the initial year compared to the subsequent year. However, the pH stabilized over time, primarily attributed to the development of a persistent biofilm layer on the concrete surface. This stable biofilm layer maintained a stable pH even as corrosion progressed deeper into the concrete (Sapkota, 2022).

4.4.2. SEM Imaging

Biogenic corrosion (**Figure 4.16**) causes a more extensive corrosion interface than chemical corrosion (**Figure 4.17**). The extensive corrosion indicates that biogenic corrosion is a more aggressive form of corrosion. Moreover, the SEM images revealed that the corrosion interface is more irregular in biogenic than chemical corrosion, suggesting that biogenic corrosion leads to more spalling and cracking than chemical corrosion.

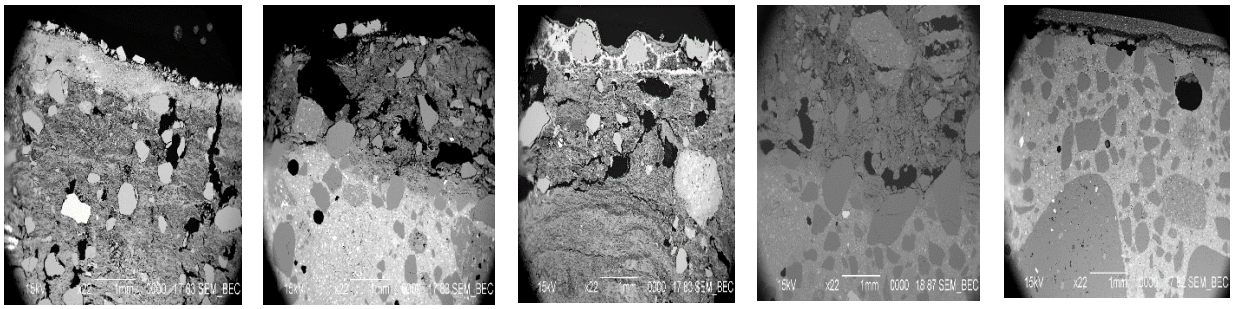

L CT **L BIO** **L ARC** **L NAN** **L EP**

Figure 4.16 *SEM Micrographs for control (CT), biocide (BIO), ARC, $NaNO_2$ (NAN), and epoxy (EP) coupons exposed to biogenic corrosion (Photo by Ray Hoff).*

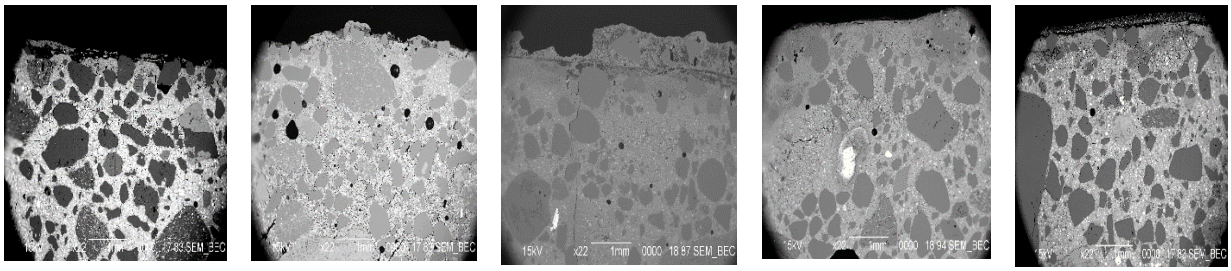

U CT **U BIO** **U ARC** **U NAN** **U EP**

Figure 4.17 *SEM Micrographs for control (CT), biocide (BIO), ARC, $NaNO_2$ (NAN), and epoxy (EP) coupons exposed to chemical corrosion (Photo by Ray Hoff).*

4.5. Synthesis of Results

Based on the results obtained from this present study and the works of Nasr (2021) and Sapkota (2022), the following observations were made regarding each test methodology.

4.5.1. ASTM C1012 Sulfate Attack

Over time, the percent strain of all the mortar bars increased for all the samples, with varying trends. The control sample expanded more than the treated samples, with the $NaNO_2$ treated samples having marginally lower strain. The ARC and biocide treated samples had a strain lower than the control samples by a statistically significant margin. As the ARC treatment decreases permeability, a decrease in strain was expected. However, biocide treatment is an admixture that should not directly affect sulfate attack resistance. Overall, the concrete was susceptible to sulfate attack, as indicated by the increasing strain throughout the exposure period.

4.5.2. ASTM C1898 Acid Attack

Over the course of 84 days, all samples, including the control and those treated with biocide, ARC, and $NaNO_2$, experienced a decrease in mass. The mortar bars and test medium exhibited discoloration and changes in appearance. The biocide treatment had the least mass loss compared to the other treatments. The $NaNO_2$ samples had a greater increase in flexural strength than the control, while the ARC and biocide increased less than the control and performed worse. Throughout the testing period, the appearance of the specimens and medium changed, with discoloration observed in all samples.

4.5.3. ASTM C1894 MICC

The effectiveness of different surface treatments in mitigating the corrosion of concrete exposed to chemical and biogenic corrosion was investigated using ASTM C1894 by Nasr (2021) and

Sapkota (2022). The results revealed that the various surface treatments had varying impacts on the resistance of concrete to MICC.

The biocide treatment proved to be the most effective in reducing the corrosion of concrete exposed to chemical and biogenic corrosion. The biocide treatment demonstrated greater effectiveness than the other treatments in reducing corrosion. It increased the density of the concrete, making it more resistant to corrosion, and reduced the permeability of the concrete, limiting the penetration of corrosive agents.

On the other hand, the ARC treatment was found to be the least effective in reducing the corrosion of concrete exposed to chemical and biogenic corrosion. The ARC treatment led to a higher surface pH of the concrete as compared with the control, which can help slow down the corrosion process. However, it did not effectively prevent the formation of biofilms on the concrete surface, which can accelerate corrosion.

The $NaNO_2$ treatment was also effective in reducing the corrosion of concrete exposed to chemical and biogenic corrosion. It created an alkaline environment on the concrete surface, making it difficult for corrosive agents to attack the concrete. Additionally, it minimized the formation of biofilms on the concrete surface.

In summary, the study results suggest that the biocide treatment is the most effective in preventing corrosion, followed by the $NaNO_2$ treatment.

During inspection, as noted by Sapkota (2022), visible corrosion was observed, which was further confirmed by changes in SUR and surface pH. The biogenic corrosion process resulted in faster neutralization of concrete compared to chemical corrosion. The acidification of the concrete occurred approximately two times faster under biogenic corrosion conditions. The biocide treatment exhibited the lowest overall SUR indication of better performance compared to

the other treatments. Also, the surface pH method demonstrates a strong correlation with the progression of MICC during stage three.

4.6. Standard Mean Difference

The standard mean differences (SMD) for various test methods and treatments were used to compare the relative performance of the treatments across the three different ASTM methods, which are summarized in **Table 4.4**. The SMD is a measure of standardized effect size that quantifies the difference between two groups, often used in meta-analyses. A positive SMD indicates that the treatment group has a higher mean compared to the control group, while a negative SMD indicates the opposite. The SMD for the control samples is zero. The larger the absolute value of the SMD, the larger the effect size, and thus, the more effective the treatment. Negative effect sizes indicate the treated samples performed worse than the control. The effectiveness of different surface treatments in mitigating microbially induced concrete corrosion can vary depending on the specific test method employed. The biocide is consistently effective across multiple test methods, except for flexural strength, while ARC and $NaNO_2$ show mixed results.

Table 4.4 *Standard Mean Difference for SUR (Sapkota, 2022), Surface pH (Sapkota, 2022), Length Change, Mass Change, and Flexural Strength compared to the control.*

Test Method	ARC	Biocide	$NaNO_2$
ASTM C1894 SUR Chemical Corrosion	0.765	0.746	0.651
ASTM C1894 SUR Biogenic Corrosion	0.373	0.504	0.223
ASTM C1894 Surface pH Chemical Corrosion	0.283	1.172	1.221
ASTM C1894 Surface pH Biogenic Corrosion	0.077	0.505	0.099
ASTM C1012 Length Change	2.110	1.985	0.927
ASTM C1898 Mass Change	-0.539	2.392	-2.128
ASTM C1898 Flexural Strength	-2.542	-1.573	1.244

From the research results conducted herein, the values for SUR, surface pH, length change, mass change, and flexural strength are compared between ARC, biocide, and $NaNO_2$ treatments and the control.

Biocide demonstrates performance better in mass change with an SMD value of 2.392, compared to ARC (-0.539) and $NaNO_2$ (-2.128). This suggests that biocide can effectively reduce the corrosion induced by the 0.005M sulfuric acid solution, leading to a lower mass change in the sample, which is an indication of better corrosion resistance. The effectiveness of biocide against sulfuric acid may increase its resistance to biogenic corrosion and maintain a higher surface pH under biogenic corrosion conditions. The effectiveness of biocide in mitigating sulfuric acid-induced corrosion and maintaining a higher surface pH under biogenic corrosion conditions has been studied. The efficacy of biocide in reducing SUR can be attributed to its ability to inhibit the growth of microorganisms that contribute to biogenic corrosion. Comparative analysis shows that the biocide treatment exhibited a higher SMD value of 0.504, indicating its superior performance compared to ARC (0.373) and $NaNO_2$ (0.223). Moreover, the biocide treatment demonstrated better performance in maintaining surface pH (0.505) during biogenic corrosion compared to ARC (0.077) and $NaNO_2$ (0.099), thereby limiting the extent of acid attack-induced damage.

In the ASTM C1012 test, the ARC samples experienced the highest SMD (2.110) compared to the other treatments, indicating higher resistance to sulfate attack. In contrast, the $NaNO_2$ samples had the lowest SMD (0.927), suggesting the least performance in sulfate resistance.

In the ASTM C1894 tests, the ARC treatment showed the highest SMD in SUR for chemical corrosion. However, it exhibited a lower SMD in surface pH for both types of corrosion, suggesting neutralization due to corrosion. The biocide and $NaNO_2$ coupons showed slower rates of change in surface pH, indicating better resistance to biogenic corrosion.

Comparing the treatments across the three tests (sulfate attack, acid attack, and simulated MICC), the ARC treatment offers better performance in sulfate resistance (ASTM C1012), while

$NaNO_2$ offers better acid resistance (ASTM C1898 Flexural Strength). In contrast, the biocide treatment exhibits better resistance to MICC (ASTM C1894). However, the ARC treatment underperforms in acid resistance tests but shows some potential in resisting MICC in the context of SUR.

Based on these results, one can conclude that the performance of the treatments varies depending on the type of corrosion they are subjected to. The $NaNO_2$ treatment seems most effective in sulfate and acid resistance, while the biocide treatment may offer better resistance to MICC. However, the treatment performance should be considered holistically, considering the specific environmental conditions and potential secondary effects of using these treatments in concrete mixtures.

The inconsistent performance of the treatments across the various tests indicate that no single treatment provided comprehensive protection against all forms of degradation. Instead, each treatment might be more effective in specific environments or against specific attacks. Therefore, selecting the appropriate concrete treatment should depend on the specific environmental conditions and the type of attack the concrete is likely to face. The MICC mechanism results in a predictable and uniform acid and sulfate corrosion environment. For effective defense against MICC, the treatment should be resistant to sulfate and acid attacks and impermeable to H_2S gas, acid, and bacteria. The results suggest enhancing resistance in these areas would provide a comprehensive solution.

5. Conclusions and Recommendations

5.1. Conclusions

The experimental investigation in the laboratory, in conjunction with the works of Nasr (2021) and Sapkota (2022), has provided valuable insights into the effectiveness of different treatments for combating MICC. It is evident that no single treatment offers comprehensive protection against all forms of degradation, and the performance of each treatment varies depending on the type of attack. From the research herein, the following conclusions can be inferred:

1. The results of the ASTM C1012 and ASTM C1898 tests suggest that the biocide, ARC, and $NaNO_2$ treatments all have the potential to reduce the expansion and mass loss of concrete when exposed to sulfate and acid solutions. The biocide was the most effective treatment, followed by the ARC coating and $NaNO_2$ treatment.
2. The flexural strength test results suggest that the $NaNO_2$ treatment was the most effective in maintaining the flexural strength of concrete exposed to the acid solution. The $NaNO_2$ sample showed a 42.87% increase in flexural strength compared to a 32.90% increase for the control samples. However, this result was not statistically significant. The ARC and biocide samples showed smaller percentage increases, with 14.32% and 13.54%, respectively.
3. The ASTM C1012 sulfate attack test results showed that the control sample and all the treated samples exhibited some degree of sulfate attack, as indicated by the increase in percent strain over 183 days. However, the samples treated with biocide, ARC, and $NaNO_2$ showed some reduction in sulfate attack compared to the control sample.
4. The ASTM C1898 acid attack test results showed that all the samples, including the control and the treated samples, experienced a reduction in mass and an increase in

flexural strength over the 84-day exposure period. The appearance of the specimens and test medium also changed, indicating an acid attack. However, only biocide was effective compared to the control with an SMD of 2.392 in terms of mass change. The $NaNO_2$ treatment showed effectiveness in improving flexural strength compared to the control, with an SMD of 1.244, but this change was not statistically significant.

5. The results indicate that while the treatments (biocide, ARC, and $NaNO_2$) did not completely prevent sulfate or acid attack on the concrete, the severity of the attacks decreased compared to the control sample in SUR, surface pH, and sulfate attack.
6. The $NaNO_2$ treatment is primarily intended to inhibit bacterial growth, but it is possible that it also has a secondary effect of improving the acid resistance of concrete. The secondary effect could be because $NaNO_2$ is a strong oxidizer, which may increase the buffer capacity of the concrete.
7. Factors beyond bacterial inhibition may have affected the flexural strength results. Unidentified variables impacted the control and $NaNO_2$ batches. Factors include environmental conditions, material composition, ARC coating degradation, and testing procedure inconsistencies.

Overall, biocide treatment is more effective than ARC and $NaNO_2$ in reducing concrete corrosion. However, treatment choice should depend on specific environmental conditions and the type of corrosion.

5.2. Recommendations for Future Research

Drawing from the findings of the study, the following recommendations can be made:

1. It should be noted that these results are based on a limited study and that further research is needed to confirm these findings. Additionally, the specific conditions of a particular treatment application may affect the effectiveness of any of these treatments.
2. Further research should be conducted to optimize the dosages and application methods of the treatments (biocide, ARC, and $NaNO_2$) to enhance their effectiveness in reducing sulfate and acid attacks on concrete, as the result contradicted the expectation, as explained in **Section 5.1**.
3. Finally, future research should consider combining different treatments (e.g., ARC and biocide) to achieve more comprehensive protection against various forms of concrete degradation.

6. References

1. Alexander, M., Bertron, A. & De Belie, N. (2013). Performance of Cement-based Materials in Aggressive Aqueous Environments: State-of-the-Art Report, RILEM TC 211-PAE" 1st ed., Springer, Ghent.
2. Alexander, M. G. & Mindess, S. (2005). Aggressive Environments and Concrete Durability in Aggregates in Concrete: Modern Concrete Technology Series, CRC Press, 2005, pp. 335-376.
3. ASTM Standard C1012 (2018). Standard Test Method for Length Change of Hydraulic-Cement Mortars Exposed to a Sulfate Solution. ASTM International, West Conshohocken, PA.
4. ASTM Standard C1894 (2019). Standard Guide for Microbially Induced Corrosion of Concrete Products. ASTM International, West Conshohocken, PA.
5. ASTM Standard C1898 (2020). Standard Test Methods for Determining the Chemical Resistance of Concrete Products to Acid Attack. ASTM International, West Conshohocken, PA.
6. ASTM Standard C1904 (2020). Standard Test Methods for Determining the Effect of Biogenic Acidification on Concrete Antimicrobial Additives and/or Concrete Products. ASTM International, West Conshohocken, PA.
7. Azzouz, M., & Al-Hashimi, H. K. (2017). Microbially induced corrosion of concrete: Mechanisms, challenges, and remediation strategies. Construction and Building Materials, 148, 122-134.

8. Bertron, J., Legrand, C., & Pigeon, M. (2014). Influence of cementitious materials on the acid resistance of concrete: An experimental study using ASTM C1898. Cement and Concrete Research, 66, 103-112. doi:10.1016/j.cemconres.2014.06.009.
9. De Schutter, G., & Audenaert, K. (2004). Evaluation of effect of cement type on concrete durability. Concrete Repair, Rehabilitation and Retrofitting, 545-550.
10. Erbektas, A. R., Isgor, O. B., & Weiss, W. J. (2019). Evaluating the efficacy of antimicrobial additives against biogenic acidification in simulated wastewater exposure solutions. RILEM Technical Letters, 4, 49–56. https://doi.org/10.21809/rilemtechlett.2019.62
11. Esnault, P., Lasseur, C., & François, P. (2013). Mitigation of microbially induced corrosion of concrete in wastewater treatment plants: A review. Water Science and Technology, 67(11), 2553-2562.
12. Ejaz, N., Hussain, J., Ghani, U., Shabir, F., Naeem, U. A., Shahmim, M. A., & Tahir, M. F. (2013). Performance of concrete under aggressive wastewater environment using differente binders. Life Sci. J, 10, 141-150.
13. Fava, J. A., & Little, D. N. (2015). Microbially induced corrosion of concrete: A review of the literature. Journal of Materials in Civil Engineering, 27(1), 04014078.
14. Foorginezhad, S., Mohseni-Dargah, M., Firoozirad, K., Aryai, V., Razmjou, A., Abbassi, R., … & Asadnia, M. (2021). Recent advances in sensing and assessment of corrosion in sewage pipelines. Process Safety and Environmental Protection, 147, 192-213.
15. Ganigue, L. A., Zhang, J., & Zhang, X. (2010). Surface treatment of concrete sewer pipe using epoxy coating for corrosion prevention. Journal of Materials in Civil Engineering, 22(10), 1071-1079.

16. Grengg, C., Mittermayr, F., Baldermann, A., Böttcher, M.E., Leis, A., Koraimann, G., Grunert, P., Dietzel, M. (2015). Microbiologically induced concrete corrosion: a case study from a combined sewer network. *Cement and Concrete Research*, 77, 16-25.
17. Grengg, C., Müller, B., Staudinger, C., Mittermayr, F., Breininger, J., Ungerböck, B., Borisov, S.M., Mayr, T. and Dietzel, M. (2019). High-resolution optical pH imaging of concrete exposed to chemically corrosive environments. *Cement and Concrete Research*, 116, pp.231-237.
18. Grengg, C., Mittermayr, F., Koraimann, G., Konrad, F., Szabo, M., Demeny, A., Dietzel, M. (2017). The decisive role of acidophilic bacteria in concrete sewer networks: a new model for fast progressing microbial concrete corrosion, *Cement and Concrete Research*, 101, 93-101.
19. Gruyaert, P., De Belie, N., & Taerwe, L. (2016). Effect of mineral additions on the acid resistance of concrete: An experimental study using ASTM C1898. Cement and Concrete Composites, 74, 1-13. doi:10.1016/j.cemconcomp.2016.02.008.
20. Gu, J.-D., Ford, T. E., Berke, N. S., & Mitchell, R. (2001). Biodeterioration of concrete by the fungus Fusarium. International Biodeterioration & Biodegradation, 47(4), 283–292.
21. Hewayde, E.E., Sattar, S.A., & Al-Rawashdeh, N.A. (2007). Evaluating the Efficiency of Microbial, Chemical and Combined Applications for controlling Sewer Corrosion. Journal of Environmental Management, 85(2), 487-493. doi:10.1016/j.jenvman.2006.09.019
22. Irassar, E. F. (2009). Sulfate attack on cementitious materials containing limestone filler—A review. Cement and Concrete Research, 39(3), 241-254.
23. Isgor, O. B., & Razaqpur, A. G. (2006). Modeling steel corrosion in concrete structures. Journal of Materials in Civil Engineering, 18(5), 698-702.

24. Islander, B.R.L., Devinny, J.S., Member, A., Mansfeld, F., Postyn, A. & Shih, H. (1991). Microbial ecology of crown corrosion in sewers." Journal of Environmental Engineering, 117, 1991, 751-770.

25. Jiang, G., Keller, J., Bond, P. L., Yuan, Z., & Pikaar, I. (2018). Effect of nitrate dosing on the microbiological sulfide oxidation in sewer systems. Water Research, 144, 492-500.

26. Jiang, G., Zhou, M., Chiu, T.H., Sun, X., Keller, J., Bond, P.L. (2016). Wastewater enhanced microbial corrosion of concrete sewers. *Environmental Science and Technology,* 50, 8084-8092.

27. Jin, Y., Zhang, X., Xu, J., & Wu, H. (2015). Experimental and numerical study of microbially induced corrosion of concrete. Construction and Building Materials, 94, 174-182.

28. Joseph, A. P., Keller, J., Bustamante, H., & Bond, P. L. (2012). Surface neutralization and H_2S oxidation at early stages of sewer corrosion: Influence of temperature, relative humidity and H_2S concentration. Water Research, 46(13), 4235–4245. https://doi.org/10.1016/j.watres.2012.05.011

29. J s h, F , P g , L , & O'Sh , J P ( ) Us f b y s evaluate the resistance of concrete to microbiologically influenced corrosion. Cement and Concrete Research, 40(10), 1551-1561. doi:10.1016/j.cemconres.2010.06.010.

30. J s h, F , P g , L , & O'Sh , J P ( ) v w f h s f h b g microbiologically influenced corrosion of concrete. Cement and Concrete Research, 43(1), 1-14.

31. Li, B., Zhang, X., Xu, J., & Wu, H. (2018). Microbially induced corrosion of concrete: A review. Construction and Building Materials, 195, 164-177.

32. Li, X., Bond, P. L., O'moore, L., Wilkie, S., Hanzic, L., Johnson, I., Mueller, K., Yuan, Z., & Jiang, G. (2020). Increased Resistance of Nitrite-Admixed Concrete to Microbially Induced Corrosion in Real Sewers. Environmental Science and Technology, 54(4), 2323–2333. https://doi.org/10.1021/acs.est.9b06680

33. Li, X., Jiang, G., Kappler, U., Bond, P. (2017). The ecology of acidophilic microorganisms in the corroding concrete sewer environment. *Frontiers in Microbiology,* 8, 683.

34. Li, X., O'Moore, L., Song, Y., Bond, P. L., Yuan, Z., Wilkie, S., Hanzic, L., & Jiang, G. (2019). The rapid chemically induced corrosion of concrete sewers at high H_2S concentration. Water Research, 162, 95–104. https://doi.org/10.1016/j.watres.2019.06.062

35. Liu, X., Wang, H., Chen, F., & Li, J. (2017). Resistance of concrete to microbiologically produced sulfuric acid: An experimental study using ASTM C1898. Construction and Building Materials, 143, 178-187. doi:10.1016/j.conbuildmat.2017.02.041.

36. Lothenbach, B., Le Saout, G., Gallucci, E., & Scrivener, K. (2008). Influence of limestone on the hydration of Portland cement. Cement and Concrete Research, 38(6), 848-860.

37. Mehta, P. K., & Monteiro, P. J. M. (2014). Concrete: Microstructure, properties, and materials (4th ed.). New York, NY: McGraw-Hill Education.

38. Montenegro, C. T., Izquierdo, M., & De Belie, N. (2012). Resistance of superabsorbent polymers to biodegradation when subjected to different exposures: soil burial and enzyme attack. Construction and Building Materials, 35, 960-969.

39. Monteny, J., Vincke, E., Beeldens, A., De Belie, N., Taerwe, L., Van Gemert, D., & Verstraete, W. (2000). Chemical, microbiological, and in situ test methods for biogenic sulfuric acid corrosion of concrete. Cement and Concrete Research, 30(4), 623-634.

40. Narasimhan, V. (2016). Microbially induced corrosion of concrete in wastewater environments. Concrete International, 38(1), 36-43.
41. Nasr, M. (2021). Mitigation of Microbially Induced Concrete Corrosion in Wastewater Infrastructure using Surface Treatments.
42. Neville, A. (2004). The confused world of sulfate attack on concrete. Cement and Concrete Research, 34(8), 1275-1296.
43. Neville, A. M. (2011). Properties of Concrete (5th ed.). New York: Pearson Education.
44. O' , M , M y, , & h s , M G ( ) P f f incorporating GGBS in aggressive wastewater environments. Construction and building materials, 27(1), 368-374.
45. Okabe, S., Odagiri, M., Ito, T., & Satoh, H. (2007). Succession of sulfur-oxidizing bacteria in the microbial community on corroding concrete in sewer systems. Applied and environmental microbiology, 73(3), 971-980.
46. Poole, A. B., & Sims, I. (Eds.). (2016). Concrete petrography: a handbook of investigative techniques. Crc Press.
47. Ramlochan, T., Zacarias, P., Hooton, R. D., & Thomas, M. D. A. (2000). The effect of pozzolans and slag on the expansion of mortars cured at elevated temperature and pressure in a sulfate solution. Cement and Concrete Research, 30(4), 585-594.
48. Sand, W., Müller, H., & Knöfel, H. (1997). Influence of concrete surface treatment on the corrosion behavior of concrete in sewage. Cement and Concrete Research, 27(11), 1717-1724.
49. Sand, W., & Bock, E. (1991). Biodeterioration of mineral materials by microorganisms — facts, fiction and perspectives. In Biodeterioration of Cultural Property.

50. Santhanam, M., Cohen, M. D., & Olek, J. (2003). Sulfate attack research—whither now?. Materials Journal, 100(1), 2-12.

51. Sapkota, R. (2022). Effectiveness of Surface Treatments on Microbial Induced Concrete Corrosion in Wastewater Infrastructure.

52. Sharma, K. R., Ganigue, R., Yuan, Z., & Pikaar, I. (2018). Iron salt dosage for sulfide control in sewers impacts the microbial community, but not corrosion rates. Water Research, 144, 126-136.

53. Sun, J., Pantazopoulou, S. J., & Banting, B. R. (2008). The role of ettringite in external sulfate attack. Cement and Concrete Research, 38(4), 557–565.

54. Sun, X., Jiang, G., Bond, P. L., Keller, J., & Yuan, Z. (2015). A novel and simple treatment for control of sulfide induced sewer concrete corrosion using free nitrous acid. Water Research, 70(0), 279–287. https://doi.org/10.1016/j.watres.2014.12.020

55. Sun, X., Jiang, G., Chiu, T. H., Zhou, M., Keller, J., & Bond, P. L. (2016). Effects of surface washing on the mitigation of concrete corrosion under sewer conditions. Cement and Concrete Composites, 68, 88–95. https://doi.org/10.1016/j.cemconcomp.2016.02.013

56. Suryavanshi, A., Scantlebury, J., & Lyon, R. (1996). C3A-AFm-CSH gel formation and its role in sulfate resistance of cement pastes. Cement and Concrete Research, 26(11), 1811-1820.

57. Taheri, S., Delgado, G. P., Agbaje, O. B., Giri, P., & Clark, S. M. (2020). Corrosion inhibitory effects of mullite in concrete exposed to sulfuric acid attack. Corrosion and Materials Degradation, 1(2), 14.

58. Thomas, M. D. A., Hooton, R. D., Scott, A., & Zibara, H. (2012). The effect of supplementary cementitious materials on chloride binding in hardened cement paste. Cement and Concrete Research, 42(1), 1-7.

59. Tikalsky, P. J., Carrasquillo, R. L., & Regan, R. P. (2004). Influence of Fly Ash on the Sulfate Resistance of Concrete. ACI Materials Journal, 87(6).

60. Wang, L., Zhang, X., & Li, B. (2016). Evaluation of the durability of concrete after exposure to biogenic acidification using ASTM C1904. Construction and Building Materials, 112, 329-336.

61. Wu, M., Wang, T., Wu, K., & Kan, L. (2020). Microbiologically induced corrosion of concrete in sewer structures: A review of the mechanisms and phenomena. Construction and Building Materials, 239, 117813. https://doi.org/10.1016/j.conbuildmat.2019.117813

62. Zaw, M. (2021). Automated Chemical Acidification Testing of Cementitious Materials.

7. Appendix

Table 7.1 *Length Change results from ASTM C1012.*

Sample Name	Description	Bar Number	Day 7	Day 14	Day 21	Day 28	Day 56
9/9/2022	Control		9/16/22	9/23/22	9/30/22	10/7/22	11/4/22
		Bar 1	-0.00200	0.00800	0.01050	0.01600	0.02500
		Bar 2	0.00500	0.01300	0.01500	0.01700	0.02850
		Bar 3	0.01100	0.01300	0.01850	0.02050	0.03150
		Bar 4	0.01000	0.01350	0.01700	0.01950	0.02800
		Bar 5	0.00850	0.01100	0.01650	0.02100	0.02850
		Bar 6	0.01050	0.01150	0.01750	0.02350	0.03350
9/10/2022		Bar 7	0.00750	0.01200	0.01650	0.01900	0.02450
		Bar 8	0.00900	0.01650	0.02000	0.02150	0.02900
		Bar 9	0.00900	0.01450	0.01800	0.02200	0.02950
		Bar 10	0.00850	0.01450	0.01650	0.01900	0.03850
		Average	0.00770	0.01275	0.01660	0.01990	0.02965
9/16/2022	Biocide		9/23/22	9/30/22	10/7/22	10/14/22	11/11/22
		Bar 1	0.00650	0.01300	0.01350	0.01500	0.02250
		Bar 2	0.00450	0.00900	0.00950	0.01200	0.02150
		Bar 3	0.00250	0.00750	0.02150	0.01250	0.01900
		Bar 4	0.00350	0.00850	0.01100	0.01400	0.02250
		Bar 5	0.00350	0.00750	0.01150	0.01250	0.02050
		Average	0.00410	0.00910	0.01340	0.01320	0.02120
9/19/2022	ARC		9/26/22	10/3/22	10/10/22	10/17/22	11/14/22
		Bar 1	-0.00650	-0.00600	0.02750	0.03150	0.03350
		Bar 2	-0.00350	-0.00800	0.02700	0.02850	0.03450
		Bar 3	0.00300	0.00700	0.00850	0.00850	0.01400
		Bar 4	0.00400	0.00650	0.00850	0.00900	0.01450
		Bar 5	0.00300	0.00500	0.00900	0.00950	0.01350
		Bar 6	0.00150	0.00600	0.01050	0.01200	0.01400
		Average	0.00025	0.00175	0.01517	0.01650	0.02067
9/22/2022	$NaNO_2$		9/29/22	10/6/22	10/13/22	10/20/22	11/17/22
		Bar 1	0.01100	0.01400	0.01300	0.01800	0.02750
		Bar 2	0.01200	0.01350	0.01550	0.01850	0.02450
		Bar 3	0.00850	0.01450	0.01650	0.01850	0.02900
		Bar 4	0.01150	0.01750	0.01750	0.01850	0.03000
		Bar 5	0.00800	0.01550	0.01650	0.01650	0.02800
		Bar 6	0.01350	0.01650	0.02050	0.02050	0.02950
		Average	0.01075	0.01525	0.01658	0.01842	0.02808

Sample Name	Description	Bar Number	Day 91	Day 105	Day 122	Day 183
9/9/2022	**Control**		**12/9/22**	**12/23/22**	**1/8/23**	**3/10/23**
		Bar 1	0.03300	0.04150	0.04850	0.07700
		Bar 2	0.03600	0.03700	0.04450	0.05950
		Bar 3	0.03650	0.04400	0.05300	0.07650
		Bar 4	0.03950	0.04000	0.04900	0.07000
		Bar 5	0.03700	0.04000	0.04700	0.07200
		Bar 6	0.04700	0.05150	0.06500	0.10600
9/10/2022		**Bar 7**	0.02100	0.03700	0.03650	0.04700
		Bar 8	0.03700	0.04000	0.04050	0.05500
		Bar 9	0.03900	0.04300	0.04700	0.06950
		Bar 10	0.03100	0.03850	0.03900	0.05400
		Average	*0.03570*	*0.04125*	*0.04700*	*0.06865*
9/16/2022	**Biocide**		**12/16/22**	**12/30/22**	**1/15/23**	**3/17/23**
		Bar 1	0.03050	0.03050	0.03050	0.03900
		Bar 2	0.02950	0.03450	0.03100	0.04000
		Bar 3	0.02600	0.03050	0.03100	0.03900
		Bar 4	0.02800	0.03150	0.03500	0.04700
		Bar 5	0.02650	0.03000	0.03000	0.03950
		Average	*0.02810*	*0.03140*	*0.03150*	*0.04090*
9/19/2022	**ARC**		**12/19/22**	**1/2/23**	**1/18/23**	**3/20/23**
		Bar 1	0.04150	0.04300	0.04100	0.04900
		Bar 2	0.04050	0.04100	0.03950	0.05300
		Bar 3	0.02050	0.02000	0.01750	0.03050
		Bar 4	0.01900	0.02050	0.01850	0.02450
		Bar 5	0.01950	0.01950	0.02050	0.02750
		Bar 6	0.01950	0.02100	0.02350	0.03650
		Average	*0.02675*	*0.02750*	*0.02675*	*0.03683*
9/22/2022	**$NaNO_2$**		**12/22/22**	**1/5/23**	**1/21/23**	**3/23/23**
		Bar 1	0.03250	0.03900	0.03700	0.04100
		Bar 2	0.03350	0.03800	0.04300	0.05050
		Bar 3	0.03650	0.04350	0.04350	0.06400
		Bar 4	0.03400	0.04150	0.04750	0.05600
		Bar 5	0.03400	0.04050	0.04050	0.06000
		Bar 6	0.03550	0.04050	0.04050	0.06100
		Average	*0.03433*	*0.04050*	*0.04200*	*0.05542*

Table 7.2 *Mass Change results from ASTM C1898.*

Description	Number of Bars (n)	Day 0 (28th day of curing)	Day 1	Day 28	Day 84
Control		**11/16/2022**	**11/17/2022**	**12/14/2022**	**2/8/2023**
	Bar A	1135.38	1135.38		
	Bar B	1152.59	1152.59		
	Bar C	1150.85	1150.85		
	Bar D	1157.42		1154.71	
	Bar E	1161.71		1162.14	
	Bar F	1161.07		1159.45	
	Bar G	1166.07			1159.59
	Bar H	1144.61			1136.59
	Bar I	1134.68			1126.92
	Average	*1151.60*	*1146.27*	*1158.77*	*1141.03*
ARC		**11/16/2022**	**11/17/2022**	**12/14/2022**	**2/8/2023**
	Bar A	1179.84	1179.84		
	Bar B	1166.00	1166.00		
	Bar C	1169.50	1169.50		
	Bar D	1186.51		1182.88	
	Bar E	1167.03		1162.45	
	Bar F	1188.84		1185.12	
	Bar G	1172.63			1165.41
	Bar H	1143.74			1138.01
	Bar I	1187.84			1171.54
	Average	*1173.55*	*1171.78*	*1176.82*	*1158.32*
Biocide		**11/23/2022**	**11/24/2022**	**12/21/2022**	**2/15/2023**
	Bar A	1171.79	1168.46		
	Bar B	1163.37	1169.01		
	Bar C	1168.84	1167.21		
	Bar D	1143.76		1143.57	
	Bar E	1173.43		1173.88	
	Bar F	1151.34		1150.33	
	Bar G	1165.50			1160.94
	Bar H	1182.30			1177.78
	Bar I	1148.00			1141.54
	Average	*1163.15*	*1168.23*	*1155.93*	*1160.09*

Description	Number of Bars (n)	Day 0 (28th day of curing)	Day 1	Day 28	Day 84
$NaNO_2$		**11/23/2022**	**11/24/2022**	**12/21/2022**	**2/15/2023**
	Bar A	1148.52	1145.48		
	Bar B	1159.15	1154.61		
	Bar C	1126.50	1120.98		
	Bar D	1110.25		1106.85	
	Bar E	1094.79		1093.48	
	Bar F	1126.90		1125.21	
	Bar G	1164.90			1153.72
	Bar H	1145.22			1136.80
	Bar I	1170.15			1158.42
	Average	*1138.49*	*1140.36*	*1108.51*	*1149.65*

Table 7.3 *Flexural Strength Results from ASTM C1898.*

Sample Name	Description	Number of Bars (n)	Day 1	Day 28	Day 84
10/19/2022	**Control**		**11/17/2022**	**12/14/2022**	**2/8/2023**
		Bar A	1049.09		
		Bar B	1306.01		
		Bar C	1300.60		
		Bar D		1502.93	
		Bar E		1455.66	
		Bar F		1123.91	
		Bar G			1689.43
		Bar H			1700.48
		Bar I			1469.76
		Average	*1218.56*	*1360.83*	*1619.89*
10/19/2022	**ARC**		**11/17/2022**	**12/14/2022**	**2/8/2023**
		Bar A	1334.46		
		Bar B	1439.67		
		Bar C	1366.40		
		Bar D		1488.69	
		Bar E		1507.47	
		Bar F		1303.00	
		Bar G			1628.48
		Bar H			1498.69
		Bar I			1606.24
		Average	*1380.18*	*1433.05*	*1577.80*
10/26/2022	**Biocide**		**11/24/2022**	**12/21/2022**	**2/15/2023**
		Bar A	1383.32		
		Bar B	1348.21		
		Bar C	1374.07		
		Bar D		1620.87	
		Bar E		1405.15	
		Bar F		1254.38	
		Bar G			1769.95
		Bar H			1497.57
		Bar I			1394.24
		Average	*1368.53*	*1426.80*	*1553.92*

Sample Name	Description	Number of Bars (n)	Day 1	Day 28	Day 84
10/26/2022	**$NaNO_2$**		**11/24/2022**	**12/21/2022**	**2/15/2023**
		Bar A	1380.64		
		Bar B	1306.33		
		Bar C	1236.69		
		Bar D		1487.76	
		Bar E		1410.09	
		Bar F		1317.29	
		Bar G			1818.60
		Bar H			1952.24
		Bar I			1834.63
		Average	*1307.89*	*1405.05*	*1868.49*

Table 7.4 *Module of Rupture.*

Sample Name	Description	Number of Bars (n)	Day 1	Day 28	Day 84
10/19/2022	**Control**		**11/17/2022**	**12/14/2022**	**2/8/2023**
		Bar A	786.82		
		Bar B	979.50		
		Bar C	975.45		
		Bar D		1127.20	
		Bar E		1091.74	
		Bar F		842.93	
		Bar G			1267.07
		Bar H			1275.36
		Bar I			1102.32
		Average	*913.92*	*1020.63*	*1214.92*
10/19/2022	**ARC**		**11/17/2022**	**12/14/2022**	**2/8/2023**
		Bar A	1000.85		
		Bar B	1079.75		
		Bar C	1024.80		
		Bar D		1116.52	
		Bar E		1130.61	
		Bar F		977.25	
		Bar G			1221.36
		Bar H			1124.02
		Bar I			1204.68
		Average	*1035.13*	*1074.79*	*1183.35*
10/26/2022	**Biocide**		**11/24/2022**	**12/21/2022**	**2/15/2023**
		Bar A	1037.49		
		Bar B	1011.16		
		Bar C	1030.55		
		Bar D		1215.65	
		Bar E		1053.86	
		Bar F		940.79	
		Bar G			1327.46
		Bar H			1123.18
		Bar I			1045.68
		Average	*1026.40*	*1070.10*	*1165.44*

Sample Name	Description	Number of Bars (n)	Day 1	Day 28	Day 84
10/26/2022	**$NaNO_2$**		**11/24/2022**	**12/21/2022**	**2/15/2023**
		Bar A	1035.48		
		Bar B	979.74		
		Bar C	927.52		
		Bar D		1115.82	
		Bar E		1057.57	
		Bar F		987.97	
		Bar G			1363.95
		Bar H			1464.18
		Bar I			1375.97
		Average	*980.91*	*1053.79*	*1401.37*